

## Article

# Combination Treatment of Retinoic Acid Plus Focal Adhesion Kinase Inhibitor Prevents Tumor Growth and Breast Cancer Cell Metastasis

Ana Carla Castro-Guijarro <sup>1</sup>, Fiorella Vanderhoeven <sup>1</sup>, Joselina Magali Mondaca <sup>2</sup>, Analía Lourdes Redondo <sup>1</sup>, Felipe Carlos Martin Zoppino <sup>3</sup> , Juan Manuel Fernandez-Muñoz <sup>3</sup> , Angel Matias Sanchez <sup>2,\*</sup>,  
and Marina Inés Flamini <sup>1,\*,†</sup>

- <sup>1</sup> Laboratorio de Biología Tumoral, Instituto de Medicina y Biología Experimental de Cuyo (IMBECU), Consejo Nacional de Investigaciones Científicas y Técnicas (CONICET), Universidad Nacional de Cuyo, Mendoza CP 5500, Argentina
  - <sup>2</sup> Laboratorio de Transducción de Señales y Movimiento Celular, Instituto de Medicina y Biología Experimental de Cuyo (IMBECU), Consejo Nacional de Investigaciones Científicas y Técnicas (CONICET), Universidad Nacional de Cuyo, Mendoza CP 5500, Argentina
  - <sup>3</sup> Laboratorio de Oncología, Instituto de Medicina y Biología Experimental de Cuyo (IMBECU), Consejo Nacional de Investigaciones Científicas y Técnicas (CONICET), Universidad Nacional de Cuyo, Mendoza CP 5500, Argentina
- \* Correspondence: amsanchez@mendoza-conicet.gov.ar (A.M.S.); mflamini@mendoza-conicet.gov.ar (M.I.F.); Tel.: +54-261-5244192 (ext. 4371) (A.M.S.); +54-261-5244152 (ext. 4371) (M.I.F.); Fax: +54-261-5244001 (A.M.S.); +54-261-5244001 (M.I.F.)
- † Contact A.M.S. and M.I.F. for reprint requests.



**Citation:** Castro-Guijarro, A.C.; Vanderhoeven, F.; Mondaca, J.M.; Redondo, A.L.; Zoppino, F.C.M.; Fernandez-Muñoz, J.M.; Sanchez, A.M.; Flamini, M.I. Combination Treatment of Retinoic Acid Plus Focal Adhesion Kinase Inhibitor Prevents Tumor Growth and Breast Cancer Cell Metastasis. *Cells* **2022**, *11*, 2988. <https://doi.org/10.3390/cells11192988>

Academic Editor: Francisco Rivero

Received: 28 May 2022

Accepted: 8 September 2022

Published: 26 September 2022

**Publisher's Note:** MDPI stays neutral with regard to jurisdictional claims in published maps and institutional affiliations.



**Copyright:** © 2022 by the authors. Licensee MDPI, Basel, Switzerland. This article is an open access article distributed under the terms and conditions of the Creative Commons Attribution (CC BY) license (<https://creativecommons.org/licenses/by/4.0/>).

**Abstract:** All-trans retinoic acid (RA), the primary metabolite of vitamin A, controls the development and homeostasis of organisms and tissues. RA and its natural and synthetic derivatives, both known as retinoids, are promising agents in treating and chemopreventing different neoplasias, including breast cancer (BC). Focal adhesion kinase (FAK) is a crucial regulator of cell migration, and its overexpression is associated with tumor metastatic behavior. Thus, pharmaceutical FAK inhibitors (FAKi) have been developed to counter its action. In this work, we hypothesize that the RA plus FAKi (RA + FAKi) approach could improve the inhibition of tumor progression. By *in silico* analysis and its subsequent validation by qPCR, we confirmed RARA, SRC, and PTK2 (encoding RAR $\alpha$ , Src, and FAK, respectively) overexpression in all breast cells tested. We also showed a different pattern of genes up/down-regulated between RA-resistant and RA-sensitive BC cells. In addition, we demonstrated that both RA-resistant BC cells (MDA-MB-231 and MDA-MB-468) display the same behavior after RA treatment, modulating the expression of genes involved in Src-FAK signaling. Furthermore, we demonstrated that although RA and FAKi administered separately decrease viability, adhesion, and migration in mammary adenocarcinoma LM3 cells, their combination exerts a higher effect. Additionally, we show that both drugs individually, as well as in combination, induce the expression of apoptosis markers such as active-caspase-3 and cleaved-PARP1. We also provided evidence that RA effects are extrapolated to other cancer cells, including T-47D BC and the human cervical carcinoma HeLa cells. In an orthotopic assay of LM3 tumor growth, whereas RA and FAKi administered separately reduced tumor growth, the combined treatment induced a more potent inhibition increasing mice survival. Moreover, in an experimental metastatic assay, RA significantly reduced metastatic lung dissemination of LM3 cells. Overall, these results indicate that RA resistance could reflect deregulation of most RA-target genes, including genes encoding components of the Src-FAK pathway. Our study demonstrates that RA plays an essential role in disrupting BC tumor growth and metastatic dissemination *in vitro* and *in vivo* by controlling FAK expression and localization. RA plus FAKi exacerbate these effects, thus suggesting that the sensitivity to RA therapies could be increased with FAKi coadministration in BC tumors.

**Keywords:** retinoids; FAK inhibitor; cell motility; metastasis; breast cancer

## 1. Introduction

All-trans-retinoic acid (RA) is a biologically active derivative of vitamin A with an established role in cell growth, differentiation, and apoptosis [1,2]. It exerts its effects through nuclear receptors called retinoic acid receptors (RARs: RAR $\alpha$ , RAR $\beta$ , and RAR $\gamma$ ), which form heterodimers with retinoid-X-receptors (RXR) to control the transcription of target genes. The transcription of more than 3000 human genes is associated with RA modulation due to retinoic acid response elements (RARE) in their promoter regions [1,3]. Inactivated RAR-RXR heterodimers form complexes with corepressors to block transcription by interfering with the access to chromatin [4]. In contrast, RA binding releases corepressors and thereby coactivators take their place to allow access to chromatin [5,6]. RA can also function via the non-genomic pathway. When RA binds to a fraction of the RARs pool present in the plasma membrane, they are rapidly and efficiently activated, resulting in the induction of multiple kinases and scaffold proteins involved in several signal transductions, thus leading to numerous effects in the cell [6].

Several studies highlight the antitumor activity of RA, particularly in the modulation of cell differentiation, metastasis, apoptosis, proliferation, migration, and invasion [7]. Due to its wide range of biological effects, RA is considered a promising anticancer drug. To date, the most successful use of RA in cancer therapy has been in the treatment of acute promyelocytic leukemia (APL) and precancerous lesions, such as leukoplakia, actinic keratosis, and cervical dysplasia [8–10]. Unfortunately, the attempt to use RA to treat the most prevalent cancers, such as breast cancer (BC), has failed, since it demonstrated controversial results [11,12]. This urges the need for studies focused on better understanding the mechanical and biological function of RA.

Metastasis is at present the leading cause of death in BC patients, it being the most challenging threat in treating advanced cancer [13,14]. The prerequisite for cancer cells to metastasize is to acquire a highly migratory and invasive phenotype. Cell migration requires the continuous and orchestrated formation and turnover of focal adhesion sites (FAs) [15]. FAs are structures involved in the attachment of cells to the extracellular matrix (ECM) and in the recruitment of cortactin, N-WASP, and Arp2/3 complex to the reorganization of actin fibers to form specialized structures that trigger cell motility [15,16]. FAs are formed by several proteins, including focal adhesion kinase (FAK), Src, paxillin, talin, vinculin, and others [15]. FAK behaves as a kinase and adapter molecule. It is considered a central regulator of cell migration since it is uniquely positioned at the convergence point of integrins and receptor tyrosine kinase signal transduction pathways, which transmit signals from the ECM to the cell cytoskeleton [17]. FAK is overexpressed in colorectal, lung, ovarian, prostate, and breast cancer, and is associated with tumor metastatic behavior [18–20].

Due to the critical role of FAK in tumorigenesis, several pharmaceutical FAK inhibitors (FAKi) have been developed and are currently being tested in clinical trials ([clinicaltrials.gov](https://clinicaltrials.gov), accessed on 28 May 2021) [21]. It has been suggested that FAKi need to be combined with other agents, as today they have not shown evidence of single-agent activity [22–24]. At present, there are no studies that focus on the combination of RA plus FAKi in BC therapy. The combination of RA and protein kinase C inhibitor has been recently suggested as a potential therapy to treat BC. These authors demonstrated prompted results of this combination in the inhibition of BC development and further encouraged the design of novel treatments employing retinoids and protein kinase inhibitors [25]. Previous research from our laboratory has demonstrated that RA inhibits adhesion and migration in BC cells [26–28], cellular processes where FAK plays a key role. Based on this, we hypothesized that the combination of RA plus FAKi (RA+FAKi) improves the treatment of advanced-stage BC patients. Thus, the aim of the present study was to determine the effect of RA administered in combination with FAKi on human BC cell adhesion and migration to further learn about signaling pathways triggered by RA, particularly in those processes that are key to the development of metastasis.

## 2. Materials and Methods

### 2.1. Cell Culture and Treatments

The human breast carcinoma cell lines SK-BR3, T-47D, MDA-MB-231 and the human cervical carcinoma cell line HeLa were obtained from the American Type Culture Collection (ATCC, Manassas, VI, USA). The murine mammary adenocarcinoma cell line LM3 was kindly provided by the Instituto de Oncología Ángel H. Roffo (Buenos Aires, Argentina) [29]. SK-BR3 and MDA-MB-231 cells were cultured in Dulbecco's Modified Eagle's Medium (DMEM), high glucose, supplemented with 10% fetal bovine serum (FBS), penicillin, and streptomycin. T-47D cells were grown in RPMI 1640 supplemented with L-glutamine, 10% FBS, penicillin, and streptomycin. LM3 cells were cultured in a minimum essential medium (MEM), supplemented with 10% FBS and gentamycin. HeLa cells were cultured in DMEM medium supplemented with 10% FBS, L-glutamine, penicillin, and streptomycin. All cell lines were maintained at 37 °C in an incubator with 5% CO<sub>2</sub>. All-trans-retinoic acid (RA) was obtained from Sigma Chemical Co (Sigma-Aldrich, St. Louis, MO, USA). RA stock solution was dissolved in dimethyl sulfoxide (DMSO) and maintained at −20 °C, protected from light in an inert atmosphere. According to our previously published results, RA was used at a final concentration of 0.1–100 µM for 72 h [26,27]. FAK inhibitor (FAKi, sc-203950) was purchased from Santa Cruz Biotechnology and was diluted in cell culture medium to the final concentration of 1–2 µM. All experiments with retinoids were performed under reduced room light conditions.

### 2.2. Bioinformatics

#### 2.2.1. Basal Gene Expression Study in Eight Cell Lines

Two microarray gene expression datasets (GSE70884 and GSE68651) were programmatically downloaded from the publicly available Gene Expression Omnibus database ([ncbi.nlm.nih.gov/geo/query/acc.cgi?acc=GSE70884](https://ncbi.nlm.nih.gov/geo/query/acc.cgi?acc=GSE70884) and [ncbi.nlm.nih.gov/geo/query/acc.cgi?acc=GSE68651](https://ncbi.nlm.nih.gov/geo/query/acc.cgi?acc=GSE68651). Accessed on 28 May 2021) using the R *GEOquery* package [30]. The first dataset consists of seven BC cell lines (MCF-7, T-47D, ZR75.1, BT-474, SK-BR3, MDA-MB-468, MDA-MB-231) with three replicates each. The second dataset is composed of three replicates of the MCF-10A cell line. The Combat method from the SVA package was used to combine the datasets into a single one and perform batch effects corrections on the expression values [31,32]. For expression profiling and differential gene expression (DGE) analysis, log<sub>2</sub> transformation of the expression values was applied. For boxplot construction, we used the same eight cell lines mentioned above and five genes involved in RA-antitumoral effects (RARA, RARB, RARG, SRC, PTK2). For the heatmap construction and cluster analysis, from the previously obtained expression matrix, five cell lines (MCF-10A, T-47D, SK-BR3, MDA-MB-468, MDA-MB-231) and 16 genes involved in different processes related to metastasis (CFL1, ACTR2, WASL, ACTR3, CDH1, VIM, MSN, TLN1, CTNNB1, VCL, DNM2, PXN, CTTN, MMP9, MMP2, and CDH2) were selected. A z-score of each gene was performed to visualize the differences in gene expression patterns between each cell line. The columns were sorted based on a hierarchical cluster with average linkage and Pearson's correlation distance. According to Silhouette dendrograms, samples were grouped into two major clusters and five minor ones representing each cell line. A differential gene expression analysis (DGE) was performed using the R *limma* package [33], comparing SK-BR3 vs. MCF-10A cell lines and T-47D vs. MCF-10A cell lines. In all cases, log<sub>2</sub> fold change values were obtained associated with the exact *p*-values.

#### 2.2.2. Gene-Expression Study in RA and Control BC Cell Lines

A gene expression dataset (GSE103426) was programmatically downloaded from the publicly available Gene Expression Omnibus database ([ncbi.nlm.nih.gov/geo/query/acc.cgi?acc=GSE103426](https://ncbi.nlm.nih.gov/geo/query/acc.cgi?acc=GSE103426). Accessed on 28 May 2021) using the R *GEOquery* package [30]. This dataset consists of two BC cell lines (MDA-MB-231, MDA-MB-468) with three replicates each, with or without RA treatment. A differential gene expression analysis (DGE) was performed using the R *limma* package [33] comparing RA treated MDA-MB-231 vs. control

MDA-MB-231 BC cell lines and the RA treated MDA-MB-468 vs. control MDA-MB-468 BC cell line. In all cases, log<sub>2</sub> fold change values were obtained associated with exact *p*-values.

### 2.3. Reverse Transcription—Quantitative PCR

Total RNA was isolated from MDA-MB-231 and T-47D cells using Trizol (Invitrogen Life Technologies, Thermo Fisher Scientific, Waltham, MA, USA) following the manufacturer's instructions. The integrity of the RNA was verified by agarose gel electrophoresis. The quantity and purity of RNA were determined by employing a NanoDrop 2000 UV/Vis spectrophotometer (Thermo Scientific, Thermo Fisher Scientific, Waltham, MA, USA). Reverse transcription was performed using a universal Oligo-dT adaptor primer and M-MLV reverse transcriptase (Moloney murine leukemia virus, Promega, Madison, WI, USA) in a thermal cycler at 37 °C for 60 min. cDNA was stored at −80 °C for further analysis. Furthermore, specific primers were designed for each gene: SRC, PTK2, VIM, CTNNA1 and CTTN. Real-time PCR was performed in triplicate for each gene, using Eva Green on Corbett Research Rotor-Gene 6000 (Qiagen, Germantown, MD, USA) with the following conditions: denaturation at 95 °C for 5 min followed by 40 cycles of denaturing and annealing. Additionally, a non-template control was included on the same run. PCR efficiencies and expression of candidates were calculated using the LinRegPCR program (version 2021.1) [34]. The relative expression of the analyzed genes was normalized to the expression of β-actin.

### 2.4. Immunoblotting

Cells were harvested in lysis buffer including 100 mM Tris-HCl (pH 6.8), 4% SDS, 20% glycerol, 1 mM Na<sub>3</sub>VO<sub>4</sub>, 1 mM NaF, and 1 mM PMSF, 1 mM PIC, 1 mM PhiC. Cell lysates were separated by SDS-PAGE and transferred into PVDF membranes. Primary antibodies used were: RARα (sc-515796), RARβ (sc-552), RARγ (sc-7387), Src (sc-5266), LDH (sc-133123), p-Paxillin (sc-365020) and Paxillin (sc-31010) from Santa Cruz Biotechnology (Santa-Cruz, CA, USA); p-FAK (BD-611807) and FAK (BD-610088) from BD Transduction Laboratories; cleaved PARP1 (ab32064) from Abcam (Cambridge, UK), active caspase-3 (bs-0081R) from Bioss. Secondary antibodies (Bioss Antibodies, Woburn, MA, USA) used were: anti-rabbit IgG-HRP (sc-2357), anti-mouse IgG-HRP (sc-358914) and anti-goat IgG-HRP (sc-2354) from Santa Cruz Biotechnology. Primary and secondary antibodies were incubated using the standard techniques. Immunodetection was accomplished using enhanced chemiluminescence and was recorded with a quantitative digital imaging system (Chemidoc XRS with Image Lab, Bio-Rad, Hercules, CA, USA).

### 2.5. Cell Adhesion Assay

Cells were exposed to RA (1–10 μM), FAKi (1 μM) or their combination RA (1 μM) plus FAKi (1 μM) for 72 h. Fifteen thousand T-47D cells/well, fifty thousand LM3 cells/well, and twenty thousand HeLa cells/well were seeded into 96-well plates previously coated with 1% sterile gelatin (Sigma-Aldrich). Cells were incubated at 37 °C for 2 h. Non-adherent T-47D cells were removed by gentle washing with PBS. The attached cells were fixed with 4% paraformaldehyde and stained with 10% ethanol/crystal violet for 20 min. Images were captured and counted in ten randomly chosen fields per well using a Nikon Eclipse E200 microscope coupled to a high-resolution CCD digital camera (Nikon, Tokyo, Japan), as previously described [26]. Cell adhesion was calculated as a percentage of attached treated cells compared to untreated cells.

### 2.6. Wound Healing Assay

A scratch wound assay was conducted to assess the influence of RA (1–10 μM), FAKi (1 μM) or their combination RA (1 μM) + FAKi (1 μM) for 72 h on cell migration. T-47D, LM3, and HeLa cells were seeded in 24-well plates and incubated until 80% confluence. Wounds were made in the monolayers by scratching the surface with a pipette tip (10 μL) as uniformly and as straight as possible. The cells were washed and the treatments were prepared. Ten μM Cytosine β-D-arabinofuranoside hydrochloride (Sigma Aldrich), an

inhibitor of DNA strand separation that prevents cell division, was added to each well. Cell migration was monitored for 72 h. Digital images from cells were taken with a 16× objective. The distance of migration was analyzed by phase-contrast microscopy and closed areas were quantified using ImageJ software. Cell migration was calculated as a percentage of migrated area in treated cells compared to untreated cells.

### 2.7. Cell Viability

The MTT [3-(4,5-dimethylthiazol-2-yl)-2,5-difeniltetrazol] (Sigma-Aldrich) was dissolved in DMSO to a final concentration of 5 mg/mL. The working solution was 0.5 mg/mL MTT. LM3 and T-47D cells were seeded into 96-well plates at a density of forty-five thousand cells/well and twenty-five thousand cells/well respectively. Treatment with RA (0.01–100 µM), FAKi (0.5–2 µM), and/or the combination of both drugs was performed. After 72 h, the medium was removed and the cells were incubated with 100 µL MTT/well for 4 h. The MTT was then removed and the formazan crystal rings were dissolved in 100 µL DMSO. Absorbance at 570 nm was measured by using a microplate reader (MULTISKAN EX; Thermo Scientific). Cell viability was calculated as a percentage of viability in treated cells compared to untreated cells.

### 2.8. Analysis of Drug Interactions

CompuSyn software was used to characterize the pharmacological interaction produced by treatments with 0.01–100 µM RA plus 0.5–2 µM FAKi in LM3 and T-47D cells. This software utilizes the combination index (CI) as a method for quantitation of synergism and antagonism in drug combinations based on the mass-action law designed by Chou and Talalay [35,36]. Synergism and antagonism were defined as a more or a less than expected additive effect, respectively. CI and affected fraction (FA) levels were calculated from the effects of varying doses on cell viability inhibition rates in the MTT assay. CI = 1 denotes an additive effect, CI < 1 indicates synergism, and CI > 1 indicates antagonism. The affected fraction (FA, range 0–1) is obtained by the following equation:  $1 - (\% \text{ survival or unaffected fraction}/100\%)$ , with 1 corresponding to 100% cell survival.

### 2.9. Cell Immunofluorescence

LM3 cells were grown on coverslips at a density of twenty thousand cells/coverslip and exposed to RA (1 µM), FAKi (1µM) or their combination RA (1 µM) + FAKi (1 µM) for 72 h. Cells were fixed with 4% paraformaldehyde for 30 min and permeabilized with 0.1% triton for 5 min. Blocking was performed with 3% bovine serum albumin for 30 min at room temperature. The cells were then incubated with an antibody against FAK (BD-610088) (BD Transduction Laboratories, Franklin Lakes, NJ, USA) overnight at 4 °C. After washing, cells were incubated with goat anti-mouse IgG-Alexa Fluor 488 (A-11001, Invitrogen) for 90 min at room temperature. The cells were then incubated with Texas Red-Phalloidin (Sigma-Aldrich) for 30 min. After washing, the nuclei were counterstained with 4'-6-diamidino-2-phenylindole (DAPI, Sigma-Aldrich), and coverslips were mounted with Vectashield mounting medium (Vector Laboratories, Burlingame, CA, USA). Immunofluorescence was visualized using a Nikon Eclipse E200 microscope and recorded with a high-resolution DP70 Olympus digital camera and examined under fluorescence microscopy (FV1000 Olympus Confocal Microscope) with a Paplon 60× lens and the FV 10-ASW 1.7 software (Olympus, Japan). To perform the quantitative analysis, we measured the mean fluorescence (total fluorescence intensity divided by the number of pixels measured, which is the parameter most similar to concentration, defining regions of interest (ROI) and performing image segmentation for protein localization quantification using ImageJ Software. Briefly, using an image of a whole-cell marker, Texas Red-Phalloidin, we generated a binary mask to define our regions of interest and measured mean fluorescence only in this section. Previously, background fluorescence was removed [37]. A minimum of 50 cells per condition were analyzed.

### 2.10. Animals

The *in vivo* studies were conducted with female BALB/c mice between two to four months old and 20–25 g in weight, purchased from the Instituto de Medicina y Biología Experimental de Cuyo (IMBECU, Mendoza, Argentina). They were randomly assigned into four groups and housed in boxes of five animals each in a climate-controlled room, with free access to food and water and a 12 h light/12 h darkness schedule. All animals were cared for following the Guiding Principles in the Care and Use of Animal of the U.S. National Institute of Health. The Institutional Animal Care and Use Committee of the School of Medical Science, Universidad Nacional de Cuyo (UNCuyo), Mendoza, Argentina (Protocol approval N°63/2015) approved all procedures.

Groups were as follows ( $n = 5$  for group, 20 animals in each independent experiment)

- (1) CONTROL (indicated as CON): animals inoculated with LM3 cells received an empty subcutaneous silastic pellet.
- (2) RA: animals inoculated with LM3 cells received a subcutaneous silastic pellet containing RA (10 mg).
- (3) FAKi: animals inoculated with LM3 cells (pretreated with FAKi) and received an empty subcutaneous silastic pellet.
- (4) RA plus FAKi (indicated as RA+FAKi): animals inoculated with LM3 cells (pretreated with FAKi) and received a subcutaneous silastic pellet containing RA (10 mg).

Animals were euthanized by cervical dislocation at the experimental endpoint or when they showed signs of suffering (human endpoint): loss of >20% of the initial weight, ulcers, or when one of the tumor diameters exceeded 10 mm. Whenever a cellular injection was performed, cell viability was higher than 95% as determined by the trypan blue exclusion test. The order of injection of different groups was randomized to eliminate any difference that may bias the outcome.

#### 2.10.1. Orthotopic Tumor Growth

Mice were injected subcutaneously into the fourth mammary gland with three hundred thousand LM3 cells, treated or not with FAKi (1  $\mu$ M for 72 h). Immediately, animals of groups 1 and 3 received an empty subcutaneous silastic pellet and the animals of groups 2 and 4 received a subcutaneous silastic pellet containing RA (10 mg). Mice were monitored daily and tumor diameters were measured twice weekly with a sliding caliper. Tumor volume was calculated with the formula  $D \times d^2/2$  (where  $d$  is the smallest diameter and  $D$  is the largest) for assessment of growth rate. Survival was monitored up to 45 days. Mice were sacrificed at the experimental endpoint (45 days post-inoculation) or when animals showed signs of suffering, such as ulcers, tumor volume greater than 10 mm and/or severe weight loss. Kaplan–Meier and log-rank tests were carried out to determine differences in survival times between experimental groups. Animals were necropsied to extract the tumors, which were fixed and embedded in paraffin for subsequent histopathological studies. These *in vivo* tests were performed in duplicate ( $n = 5$  per group), with 20 animals in each independent experiment.

#### 2.10.2. Experimental Lung Metastasis Assay

The animals of groups 1 and 3 received an empty subcutaneous silastic pellet and the animals of groups 2 and 4 received a subcutaneous silastic pellet containing RA (10 mg). After a week, mice were inoculated in the tail vein with three hundred thousand LM3 cells, pretreated or not with FAKi (1  $\mu$ M for 72 h). Twenty-one days post-inoculation of tumor cells, mice were euthanized and necropsied. The lungs were ablated and fixed in Bouin's solution to record the number of superficial lung nodules in each case under a dissecting microscope. These *in vivo* tests were performed in duplicate  $n = 5$  per group, with 20 animals in each independent experiment.

### 2.11. Histological Analysis

For immunohistochemistry, orthotopic tumors were fixed in 4% formalin, embedded in paraffin and 4  $\mu$ m sections were mounted on glass slides. Antigen unmasking was carried out in a 0.01 M citrate buffer (pH 6.0) at 100 °C for 30 min. Endogenous peroxidase activity was reduced by 30 min incubation with hydrogen peroxide (0.01%). The blockade was carried out with 10% skim milk for 1 h. The primary antibody Ki-67 (15,580, Abcam) was incubated overnight at 4 °C. As a detection method, we used the biotin-streptavidin-peroxidase system. Diaminobenzidine was used as a chromogen substrate. Slides were lightly counterstained with hematoxylin and observed with an Eclipse E400 microscope (Nikon). We analyzed five randomly selected samples from each group. Five fields were randomly considered for scoring. A minimum of 500 cells per tissue were counted.

### 2.12. Statistical Analysis

Statistical analysis of the data was performed with one-way analysis of variance (ANOVA) followed by Tukey-Kramer Multiple-Comparisons or Kruskal-Wallis test using GraphPad Prism 5.03 software (San Diego, CA, USA). The Kaplan-Meier and log-rank tests were used to estimate survival time after treatments and to compare experimental groups.  $p < 0.05$  was considered statistically significant. All values were expressed as mean  $\pm$  standard error (SD) of three independent experiments. All bioinformatics analyses were performed using R version 4.0.4 in a Windows environment with Intel Core i7 with 32 GB of RAM (Chandler, AZ, USA).

## 3. Results

### 3.1. Differential Gene Expression Analysis of Cancer-Related Genes among BC Cells

Published results of different trials show that the use of retinoids in BC patients has controversial results. Taking into account that RA exerts its effects via RARs and that Src-FAK are critical proteins involved in cancer progression, we initially explored the expression profiles of RARA, RARB, RARG, SRC, and PTK2 in different types of human BC cells (T-47D, MCF7, ZR75.1, BT-474, SK-BR3, MDA-MB-468, and MDA-MB-231) and a normal breast cell line (MCF-10A). For this purpose, we performed a transcriptome analysis using two datasets from the publicly available Gene Expression Omnibus database (GSE70884 and GSE68651). We found that RARA (RAR $\alpha$ ), SRC (Src), and PTK2 (FAK) are highly expressed in all breast cells. MDA-MB-231 and SK-BR3 have the lowest and highest level of RARA expression, respectively. RARB and RARG are expressed at similarly low levels in all breast cell lines (Figure 1A).

We next compared the expression of sixteen genes between RA-resistant (MDA-MB-231 and MDA-MB-468), RA-sensitive (SK-BR3 and T-47D) BC cells, and a normal breast cell line (MCF-10A). This set of genes was selected since they are biomarkers of different processes involved in BC metastasis such as MSN (moesin), CFL1 (cofilin) (*actin cytoskeleton remodeling/depolymerization process*); VCL (vinculin), TLN1 (talin), PXN (paxillin), DNM2 (dynamin) (*FAs dynamics*); CTTN (cortactin), WASL (family of the Wiskott Aldrich Syndrome Proteins, WASP), ACTR2 (Arp2 subunit), ACTR3 (Arp3 subunit) (*actin nucleation*); CDH1 (cadherin-1), VIM (vimentin), CDH2 (cadherin-2), CTNNB1 ( $\beta$ -catenin) (*Epithelial-Mesenchymal Transition, EMT*); and MMP2, MMP9 (matrix metalloproteinases 2 and 9) (*invasion/extracellular matrix disassembly*). All samples were sorted based on a hierarchical cluster algorithm with average linkage and Pearson's correlation distance. According to Silhouette dendrograms, analysis samples were grouped into two major clusters. In one branch, it groups MDA-MB-231 and MDA-MB-468 (RA-resistant) cell lines; in the other, it groups SK-BR3, T-47D (RA-sensitive), and MCF-10A (normal) cell lines. Figure 1B shows genetic similarities between RA-resistant BC cell lines and, on the other hand, between RA-sensitive BC cell lines and the normal ones. In general, the selected genes show low expression in normal and RA-sensitive cells compared to the same genes that are over-expressed in RA-resistant cells. Furthermore, we observed that the expression of VIM, MSN, TLN1, and CTNNB1 is markedly different between RA-sensitive and RA-resistant BC

cells. In RA-resistant cells, these genes are overexpressed; meanwhile, in RA-sensitive cells, they are underexpressed. We noted that the expression of these genes is similar between RA-sensitive cells and the normal breast cell line MCF-10A (Figure 1B, genes marked in blue). MMP9 expression is low in RA-resistant compared with RA-sensitive and normal lines (Figure 1B). Additionally, we found that the expression of CTTN and CDH2 is overexpressed in RA-resistant and normal breast cells compared to RA-sensitive (Figure 1B, genes marked in orange). Altogether, this suggests that VIM, MSN, TLN1, CTNNB1, CTTN, MMP9, and CDH2 are promising candidates to be studied as markers of RA response. Bioinformatics data were validated measuring SRC, PTK2, VIM, CTNNB1 and CTTN by qPCR in control T-47D (RA-sensitive) and MDA-MB-231 (RA-resistant) BC cells (Figure 1C).

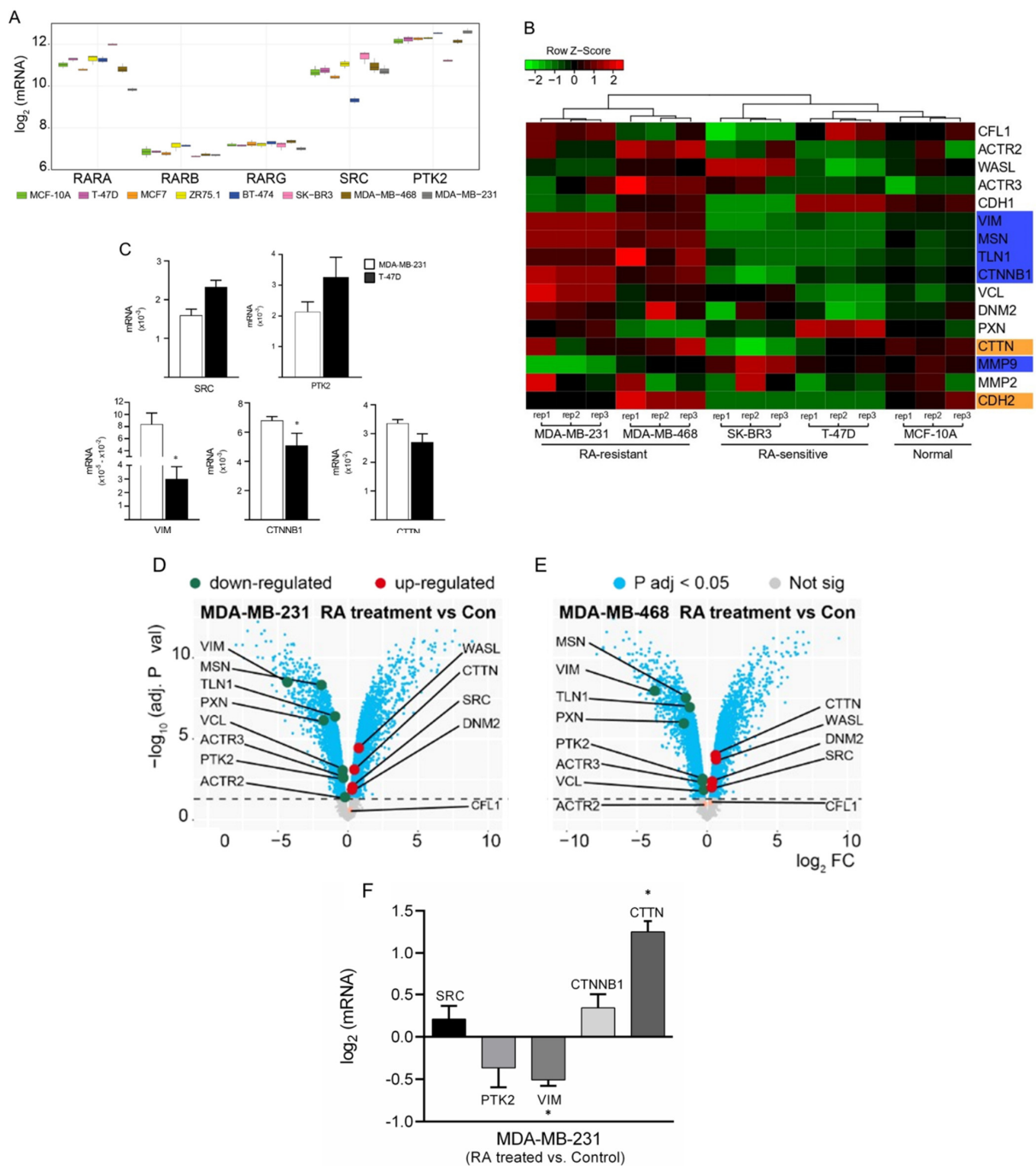


**Figure 1.** Expression of genes involved in metastasis process in a panel of BC cells. (A) Boxplot showing the gene expression patterns of five genes of interest: RARA, RARB, RARG, SRC, and PTK2

(encoding RAR $\alpha$ , RAR $\beta$ , RAR $\gamma$ , Src, and FAK respectively). Each color represents a breast cell line (MCF-10A, MCF-7, T-47D, ZR75.1, BT-474, SK-BR3, MDA-MB-468, MDA-MB-231). **(B)** Gene expression heatmap of 16 genes involved in different processes related to metastasis. The MCF-10A, T-47D, SK-BR3, MDA-MB-468, and MDA-MB-231 cell lines were used. Expression patterns of genes are represented in a green-red scale where low expression levels are in green and high expression levels in red. By a hierarchical clustering algorithm, samples were grouped into two major clusters and five minor ones that represent each cell line. **(C)** SRC, PTK2, VIM, CTNNB1 and CTTN expression in T-47D and MDA-MB-231 cells was validated with qPCR. Normalization was done with respect of the expression of  $\beta$ -actin. qPCR was performed in triplicate for each gene. \* =  $p < 0.05$  vs. MDA-MB-231 cells **(D,E)** Volcano plots of differential gene expression analysis achieved by limma R method. In the  $x$ -axis the  $\log_2$  fold change (FC) of RA-treated MDA-MB-231 vs. control MDA-MB-231 BC cell; and RA-treated MDA-MB-468 vs. control MDA-MB-468 BC cell. Genes with adjusted  $p$ -value  $< 0.05$  are indicated above the horizontal dashed line. Upregulated genes are shown in red and down-regulated genes are shown in green. **(F)** SRC, CTNNB1, CTTN, PTK2 and VIM expression was normalized with  $\beta$ -actin. In the  $x$ -axis the  $\log_2$  fold change of RA-treated MDA-MB-231 vs. control MDA-MB-231. qPCR was performed in triplicate for each gene.

To further elucidate whether genes are associated with RA-resistance, we performed a differential gene expression analysis in control and RA-treated MDA-MB-468 and MDA-MB-231 BC cells. In Figure 1D,E, both cells show the same behavior. RA administration (100 nM, 18 h) modulated the expression of all the genes analyzed, except ACTR2 and CFL1. Genes like WASL, CTTN, SRC, and DNMT2 were upregulated (Figure 1D,E, *genes marked in red*), while VIM, MSN, TLN1, PXN, VCL, ACTR3, and PTK2 were downregulated (Figure 1D,E, *genes marked in green*). We confirmed by qPCR that in MDA-MB-231 cells the administration of 100 nm RA during 18 h upregulated the expression of SRC, CTNNB1 and CTTN while PTK2 and VIM were downregulated (Figure 1F).

These results suggest that RA-resistance would reflect the deregulation of most RA-target genes, mainly those encoding components from the signaling of the Src-FAK pathway.

We also examined the differential gene expression between SK-BR3/T-47D and normal mammary cell line MCF-10A. We used a gene expression dataset from the publicly available Gene Expression Omnibus database (GSE103426). The volcano diagrams show that both BC cells exhibit a decreased expression of VIM, CDH2, and MSN compared to MCF-10A (Supplementary Figure S1, *genes marked in green*). We also found that SK-BR3 has an increased expression of RARA, WASL, SRC, and MMP9 compared to MCF-10A (Supplementary Figure S1A, *genes marked in red*), while T-47D has an increased expression of CDH1 and PXN (Supplementary Figure S1B, *genes marked in red*).

### 3.2. RA Reduces Cell Adhesion and Migration in Tumoral Cells

To confirm the role of RA in inhibiting tumor progression, we first verified the expression of RARs, Src, and FAK in T-47D, SK-BR3, and LM3 by western blot analysis. We found that RAR $\alpha$ , RAR $\beta$ , RAR $\gamma$ , Src, and FAK were present in all BC cell lines analyzed (Figure 2A and Supplementary Figure S2).

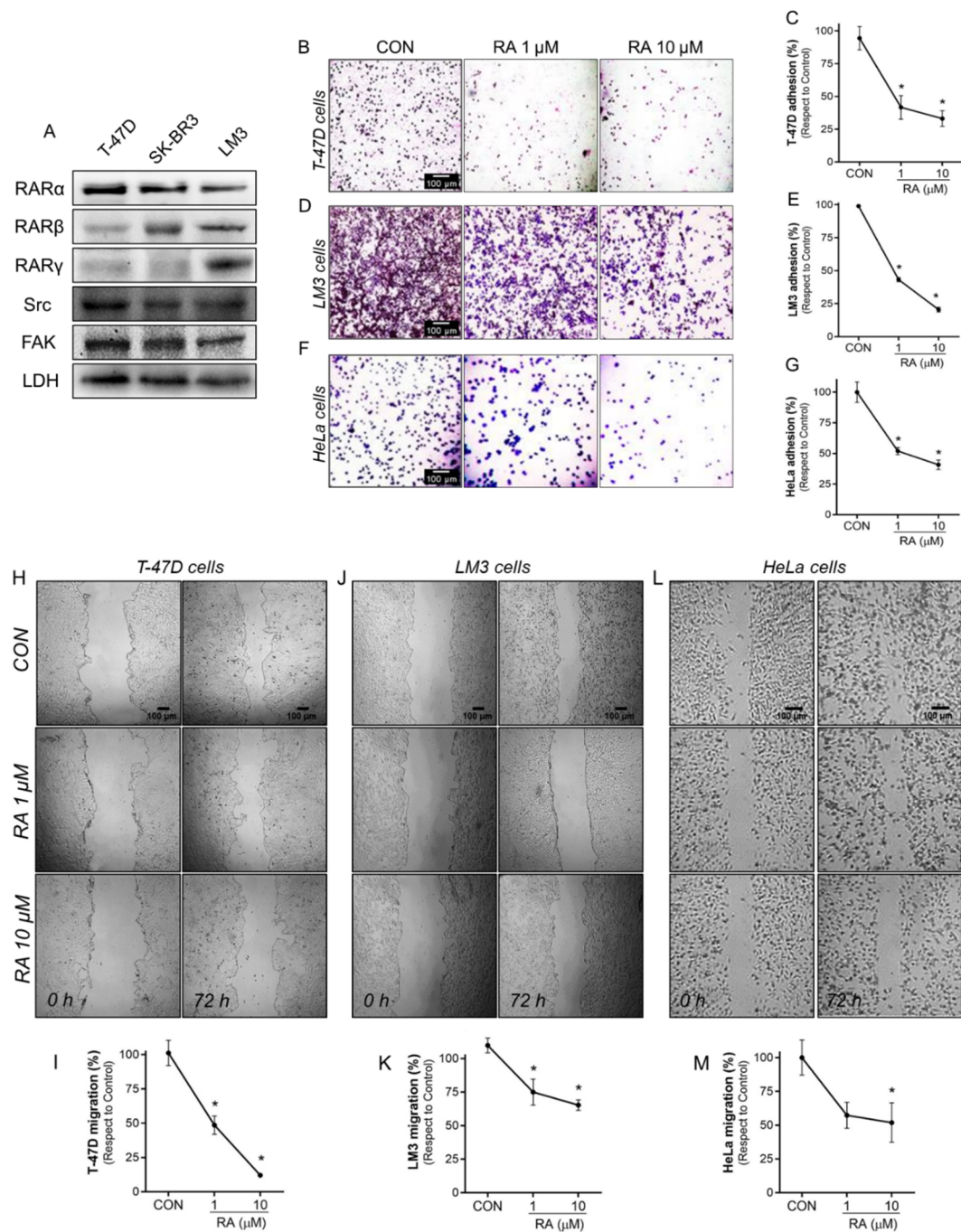


**Figure 2.** RA reduces cancer cell adhesion and migration. (A) Whole-cell lysates from human BC cell lines T-47D, SK-BR3, and a murine BC cell line LM3 were evaluated to determine the expression of RAR $\alpha$ , RAR $\beta$ , RAR $\gamma$ , Src and FAK by western blot assay. LDH expression was used as a protein loading control. A representative blot is shown. (B,C) T-47D, (D,E) LM3, and (F,G) HeLa cells were treated with RA (1–10  $\mu$ M) treatment for 72 h. After the treatment, cells were seeded into 96-well plates previously covered with gelatin and a cell adhesion assay was performed. Representative images and percentages of adhered cells are shown. (H,I) T-47D, (J,K) LM3 and (L,M) HeLa cells were exposed to RA (1–10  $\mu$ M) for 72 h and cell migration by wound-healing assay was performed. Representative images are shown. Gap closure was quantified by the use of the ImageJ software. Adhesion and migration values are presented as a percentage of control. \* =  $p < 0.05$  vs. control, CON. All experiments were performed in triplicates with consistent results.

Then, we evaluated the RA effect on cell adhesion and migration in human T-47D and murine LM3 BC cell lines. In both models, treatment with RA (1–10  $\mu\text{M}$ ) for 72 h markedly decreased cell adhesion to an extracellular matrix-like surface by 58–79%, respectively, compared to the control group (Figure 2B–E). Likewise, the administration of RA (1–10  $\mu\text{M}$ ) during 72 h reduced cell migration by 52–88% in T-47D and by 25–35% in LM3 cells (Figure 2H–K). Furthermore, we noted that RA inhibitory effects are extrapolated to other cancer cells. Treatment with RA (1–10  $\mu\text{M}$ ) for 72 h in the human cervical carcinoma cell line HeLa significantly inhibited cell adhesion (Figure 2F,G) and migration (Figure 2L,M) in a dose-dependent manner.

### 3.3. Treatment with RA Plus FAKi Reduces RAR $\alpha$ , FAK, and Paxillin Expression Decreasing LM3 Cells Viability via Caspase-3 and PARP1 Cleavage

Due to the fundamental role of RA and FAK in tumor progression, we next evaluated whether the combined treatment of RA with the specific inhibitor of FAK (FAKi) improves the inhibition of tumorigenesis. First, we tested the sensitivity of LM3 and T-47D to drugs. We performed an MTT assay using a dose range of RA (0.01–100  $\mu\text{M}$ ) and FAKi (0.5–2  $\mu\text{M}$ ) and their combinations for 72 h. We observed that all doses of RA treatment decreased cell viability in both cell lines, meanwhile treatment with FAKi only decreased 38% of cell viability at the highest concentration (2  $\mu\text{M}$ ) in LM3 cells. We noted that LM3 cells are more sensitive to RA and FAKi than T-47D cells. A synergistic effect was observed in the inhibition of cell viability when combined treatments were administered at the highest concentration in LM3 and T-47D cells (Figure 3A,M). Compusyn software was then used to examine the degree of drug interaction when treating cells with both drugs simultaneously. The results indicated that RA+FAKi exerted a synergistic effect when 77% and 87% of cell growth inhibition was reached at the highest concentration tested in LM3 and T-47D cells, respectively, associated with a CI inferior to 1, as shown in Supplementary Figure S3. This implies that the interaction between the two drugs produced a more significant effect than expected for the sum of the treatments.

Next, to further study the anti-proliferative effects of RA and FAKi; LM3 and T-47D cells were treated for 72 h with RA (1  $\mu\text{M}$ ), FAKi (1–2  $\mu\text{M}$ ), and their combinations and the expression of RARs, FAK, paxillin and the apoptotic markers active caspase-3 and cleaved PARP1 were analyzed. In LM3 cells, we found that all treatments induced the downregulation of RAR $\alpha$ , FAK, and paxillin compared to the control. The RA + FAKi combinations resulted in higher downregulation than RA alone (Figure 3B,C,F,G). On the other hand, we observed that the administration of RA induced the upregulation of RAR $\beta$ , while the treatment with FAKi (2  $\mu\text{M}$ ) decreased its expression compared to the control group. Moreover, RA + FAKi reduced RAR $\beta$  expression compared to RA but did not affect its expression compared to the control (Figure 3B,D). Additionally, RA and FAKi reduced RAR $\gamma$  expression as a single agent; however, their combinations did not affect it (Figure 3B,E).

Regarding apoptosis, we observed that in LM3 and T-47D cells, RA, FAKi (2 $\mu\text{M}$ ) and the combined treatments induced an increase in apoptosis markers of active caspase-3 and cleaved PARP1 compared to control cells; the combined treatment did not enhance this effect (Figure 3H,K,L,N,Q,R).

Since the action of FAK inhibitors blocks the specific autophosphorylation and activation of FAK kinase, we investigated whether inhibition with FAKi blocks the downstream pathway of FAK. We therefore analyzed the phosphorylation of FAK and its target protein, paxillin. We confirmed that in LM3 and T-47D cells, FAKi (2  $\mu\text{M}$ ) and both RA + FAKi combined treatments reduced FAK and paxillin's phosphorylation and consequent activation (Figure 3H–J,N–P). This suggest that the inhibition of FAK and paxillin persist during long periods of time.

We also performed an immunofluorescence assay on LM3 cells treated with RA (1  $\mu\text{M}$ ), FAKi (1  $\mu\text{M}$ ), and their combination for 72 h to reveal the expression and subcellular localization of FAK. We visualized that FAK is homogeneously and diffusely localized throughout

the cytoplasm in control cells, whereas treatment with RA and RA + FAKi triggers FAK nuclear relocalization (Figure 3S and Figure S4). This was associated with a significant increase of nuclear FAK intensity, quantified by analyzing the pixel intensity in a line including the cell cytoplasmic and nuclear areas (Figure 3S, boxes). Furthermore, we observed in all treatments the longitudinal arrangement of actin fibers, typical characteristics of a static cell phenotype, suggesting that drug administration affects the reorganization of the actin cytoskeleton (Figure 3S and Figure S4), preventing the cell from being able to drive its motor machinery impairing BC cell motility. In parallel, we also confirmed that the combined treatment significantly reduced FAK expression (mean intensity, pixel/area) (Figure 3T).

LM3 Cells

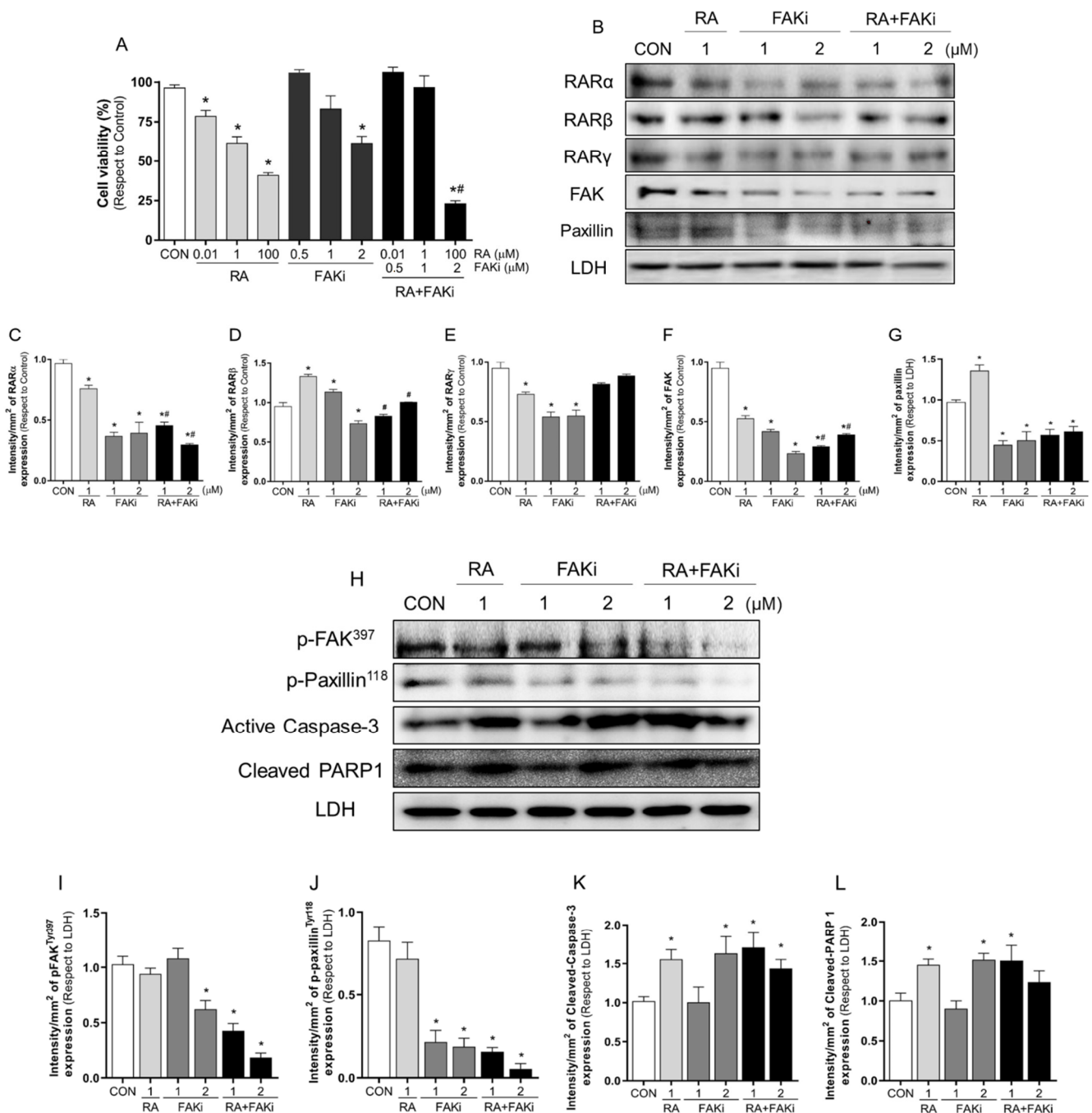
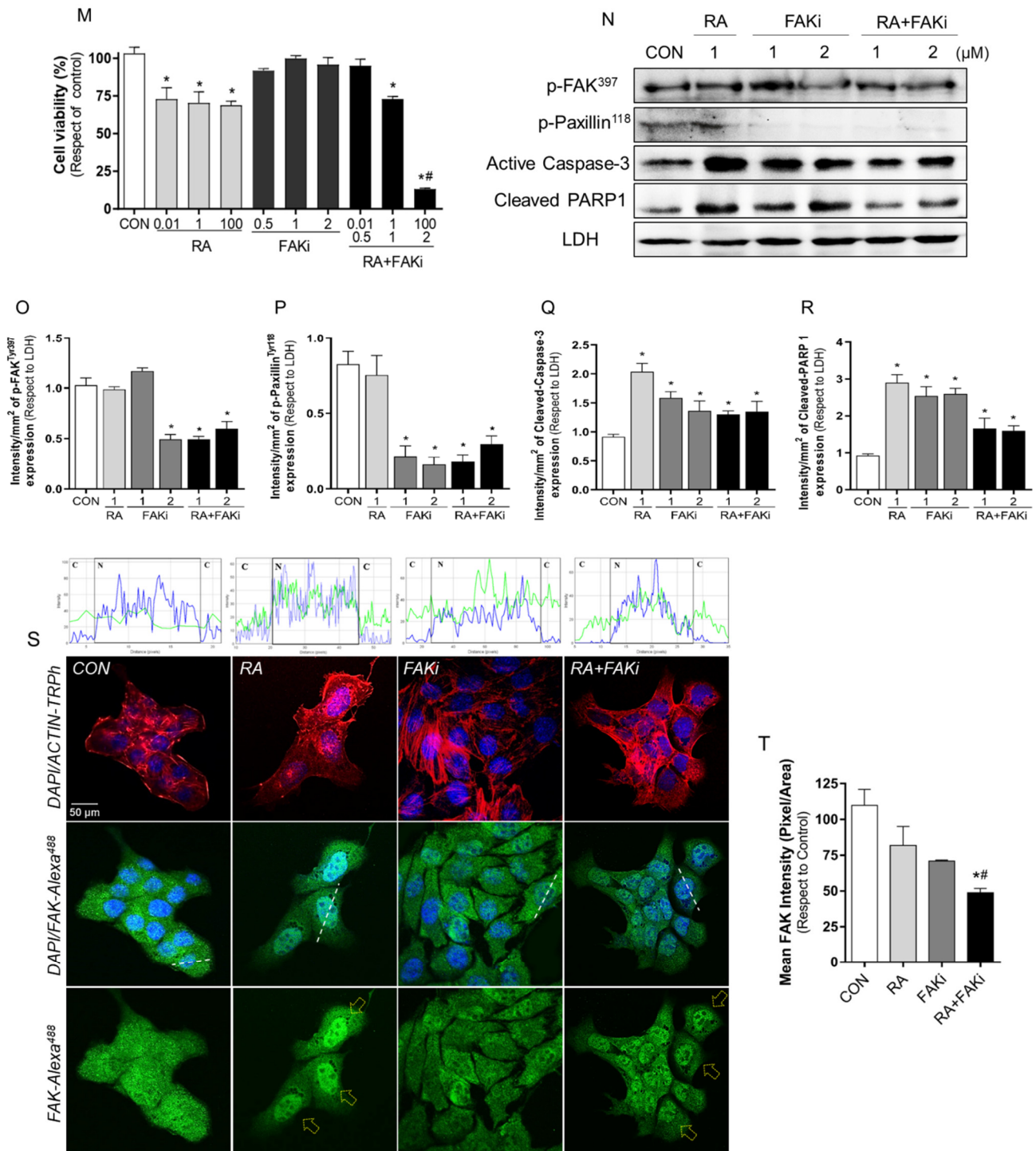


Figure 3. Cont.

T-47D Cells



**Figure 3.** LM3 and T-47D cells viability and apoptosis. (A) LM3 cells were treated with increasing doses of RA (0.01–100 μM), FAKi (0.5–2 μM), and their combinations (0.01 μM RA + 0.5 μM FAKi), (1 μM RA + 1 μM FAKi) and (100 μM RA + 2 μM FAKi) for 72 h. The results were expressed as a percentage (%) of surviving cells compared to the control (CON, 100% survival). (B) LM3 cells were exposed with RA (1 μM), FAKi (1–2 μM) and their combinations (1 μM RA + 1 μM FAKi), (1 μM RA + 2 μM FAKi) for 72 h, and expression of RARα, RARβ, RARγ, FAK and Paxillin were analyzed by western blot assay. LDH expression is shown as a loading control. (C–G) Densitometric quantifications of RARα, RARβ, RARγ, FAK and Paxillin bands. Intensity values were adjusted to

the corresponding intensity values of LDH and then normalized to the control. (H) LM3 cells were exposed with RA (1  $\mu$ M), FAKi (1–2  $\mu$ M) and their combinations (1  $\mu$ M RA + 1  $\mu$ M FAKi), (1  $\mu$ M RA + 2  $\mu$ M FAKi) for 72 h and expression of p-FAK<sup>Tyr397</sup>, p-Paxillin<sup>Tyr118</sup>, active caspase-3 and cleaved PARP1 were analyzed by western blot assay. LDH expression is shown as a loading control. (I–L) Densitometric quantifications of p-FAK<sup>Tyr397</sup>, p-Paxillin<sup>Tyr118</sup>, active caspase-3 and cleaved PARP1 bands. Intensity values were adjusted to the corresponding intensity values of LDH and then normalized to the control. (M) T-47D cells were treated with increasing doses of RA (0.01–100  $\mu$ M), FAKi (0.5–2  $\mu$ M), and their combinations (0.01  $\mu$ M RA + 0.5  $\mu$ M FAKi), (1  $\mu$ M RA + 1  $\mu$ M FAKi) and (100  $\mu$ M RA + 2  $\mu$ M FAKi) for 72 h. The results were expressed as a percentage (%) of surviving cells compared to the control (CON, 100% survival). (N) T-47D BC cells were exposed with RA (1  $\mu$ M), FAKi (1–2  $\mu$ M) and their combinations (1  $\mu$ M RA + 1  $\mu$ M FAKi), (1  $\mu$ M RA + 2  $\mu$ M FAKi) for 72 h and expression of p-FAK<sup>Tyr397</sup>, p-Paxillin<sup>Tyr118</sup>, active caspase-3 and cleaved PARP1 were analyzed by western blot assay. LDH expression is shown as a loading control. (O–R) Densitometric quantifications of p-FAK<sup>Tyr397</sup>, p-Paxillin<sup>Tyr118</sup>, active caspase-3 and cleaved PARP1 bands. Intensity values were adjusted to the corresponding intensity values of LDH and then normalized to the control. (S) LM3 cells were exposed to RA (1  $\mu$ M), FAKi (1 $\mu$ M) or their combinations (1  $\mu$ M RA + 1  $\mu$ M FAKi) for 72 h. An immunofluorescence assay was performed, murine cells were stained with anti-FAK linked to Alexa Fluor 488 (green), filamentous actin was stained with phalloidin linked to Texas Red (red), and nuclei were counterstained with DAPI (blue). The images were examined under fluorescence microscopy (FV1000 Olympus Confocal Microscope). The dotted white line on the cells indicates the area analyzed in the graphs. The y-axis displays the intensity of fluorescence and the x-axis shows the pixels. C (cytoplasmic) and N (nuclear) areas indicate the parts of the graph corresponding to the cytoplasmic and nuclear areas. Fluorescent intensity levels are represented in blue (DAPI, nucleus) and green (FAK- Alexa488). Yellow arrows indicate nuclear FAK re-localization. (T) Quantification of mean FAK intensity in pixels per area in the different conditions. Results are expressed as a percentage of mean FAK intensity  $\pm$  SD compared to the control cells. \* =  $p < 0.05$  vs. control, CON. # =  $p < 0.05$  vs. RA. Representative images are shown. All experiments were performed in triplicate with consistent results; representative images are shown.

#### 3.4. RA and FAKi Combination Improve LM3 Adhesion and Migration Inhibition

We tested the ability of LM3 cells to adhere to an ECM substrate after RA (1  $\mu$ M), FAKi (1  $\mu$ M), and their combination over 72 h. We showed that treatment with RA, FAKi, and RA + FAKi reduced cell adhesion compared to the control. The RA plus FAKi produced a more significant inhibition than RA alone (Figure 4A,B). In parallel, we exposed cells to RA, FAKi, and RA + FAKi and we monitored cell motility for 72 h. We found a significant inhibition of cell migration in all conditions tested compared to the control, reaching the major inhibition of migration in the combined treatment (Figure 4C,D).

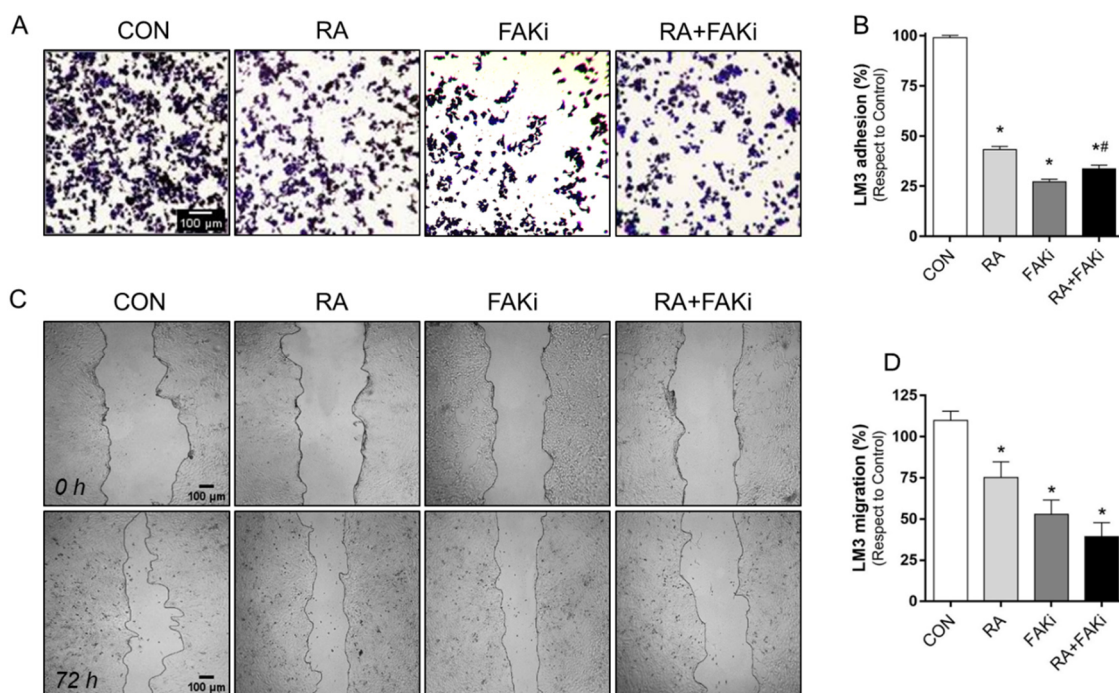


**Figure 4.** RA plus FAKi controls LM3 cell adhesion and migration. LM3 cells were treated with 1  $\mu$ M RA, 1  $\mu$ M FAKi or their combinations 1  $\mu$ M RA + 1  $\mu$ M FAKi for 72 h and cell adhesion and migration assay was performed. (A,B) Representative images and percentages of LM3 cells adhered to gelatin and (C,D) LM3 cell migration are shown. The gap closure was quantified by the use of ImageJ software. Adhesion/migration results were expressed as a percentage of attached/migrated cells vs. control cells, CON. \* =  $p < 0.05$  vs. control, CON. # =  $p < 0.05$  vs. RA. Measures are from three independent experiments.

### 3.5. RA Plus FAKi Reduces Tumor Growth and Metastasis, Increasing Mice Survival

Finally, we performed a murine in vivo model to determine correlation with the in vitro results. Tumor growth was evaluated by the orthotopic tumor growth assay consisting of inoculating murine LM3 cells, treated or not with FAKi (1  $\mu$ M, 72 h), in the mammary gland BALB/c mice bearing RA or not bearing it (10 mg)-subcutaneous pellet. We observed reduced tumor growth in animals that received RA systemically through a slow-release pellet (RA group), and animals where FAK was pharmacologically inhibited (FAKi group); however, in the combined treatment, RA + FAKi induced a more potent inhibition in tumor volume (Figure 5A,B). In accordance with this, RA and FAKi treatment increased mice survival, but only the combination RA + FAKi was statistically significant (Figure 5C). In addition, we observed that in controls and in the FAKi group the tumors were histopathologically aggressive, even ulcerating the dermis. In these groups the tumor diameters exceeded 10 mm before 45 days of the experimental endpoint and therefore the animals had to be sacrificed because of the human endpoint. The treatment with RA and the combination RA + FAKi prevented the development of these highly proliferative tumors. Representative images of ulcers found in control animals (Figure 5D,E,H) and tumors of combined treatments are shown (Figure 5F,G). The total body weight of mice was not different in the experimental groups compared to control (Supplementary Figure S5).

On the other hand, since Ki-67 is widely used in routine pathology as an established biomarker of cell division, to assess the proliferation rate of human BC tumors, we measured Ki-67 expression by immunohistochemistry in mice tumors. We found that the percentage of positive cells for Ki-67 was markedly lower in the treatments with FAKi and RA + FAKi compared to the control group (Figure 5I,J).

Finally, we performed an experimental metastatic assay to analyze the effect of the RA + FAKi combination on the spread of tumor cells. LM3 cells, pretreated or not with

FAKi (1  $\mu$ M, 72 h), were injected into the tail vein of mice bearing RA or not (10 mg) silastic pellet. We found that RA significantly reduced metastatic lung dissemination. FAKi and the RA + FAKi combination presented a lower but non-significant number of lung nodules than the control group (Figure 5K,L).

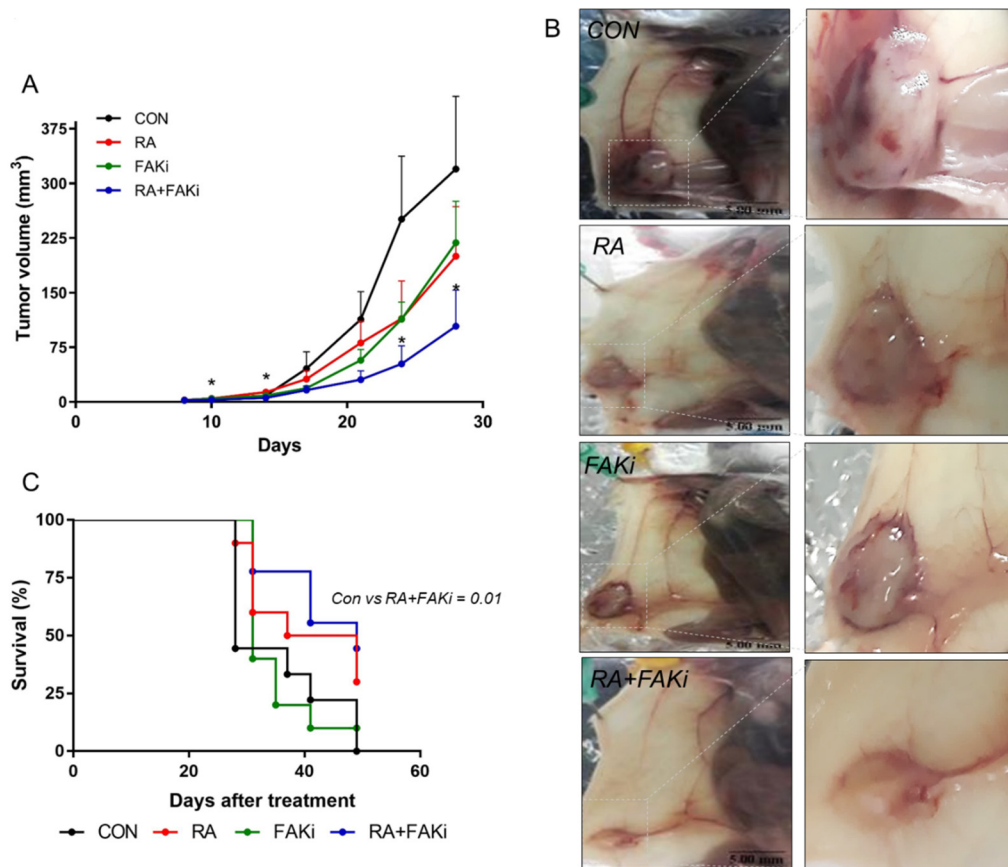
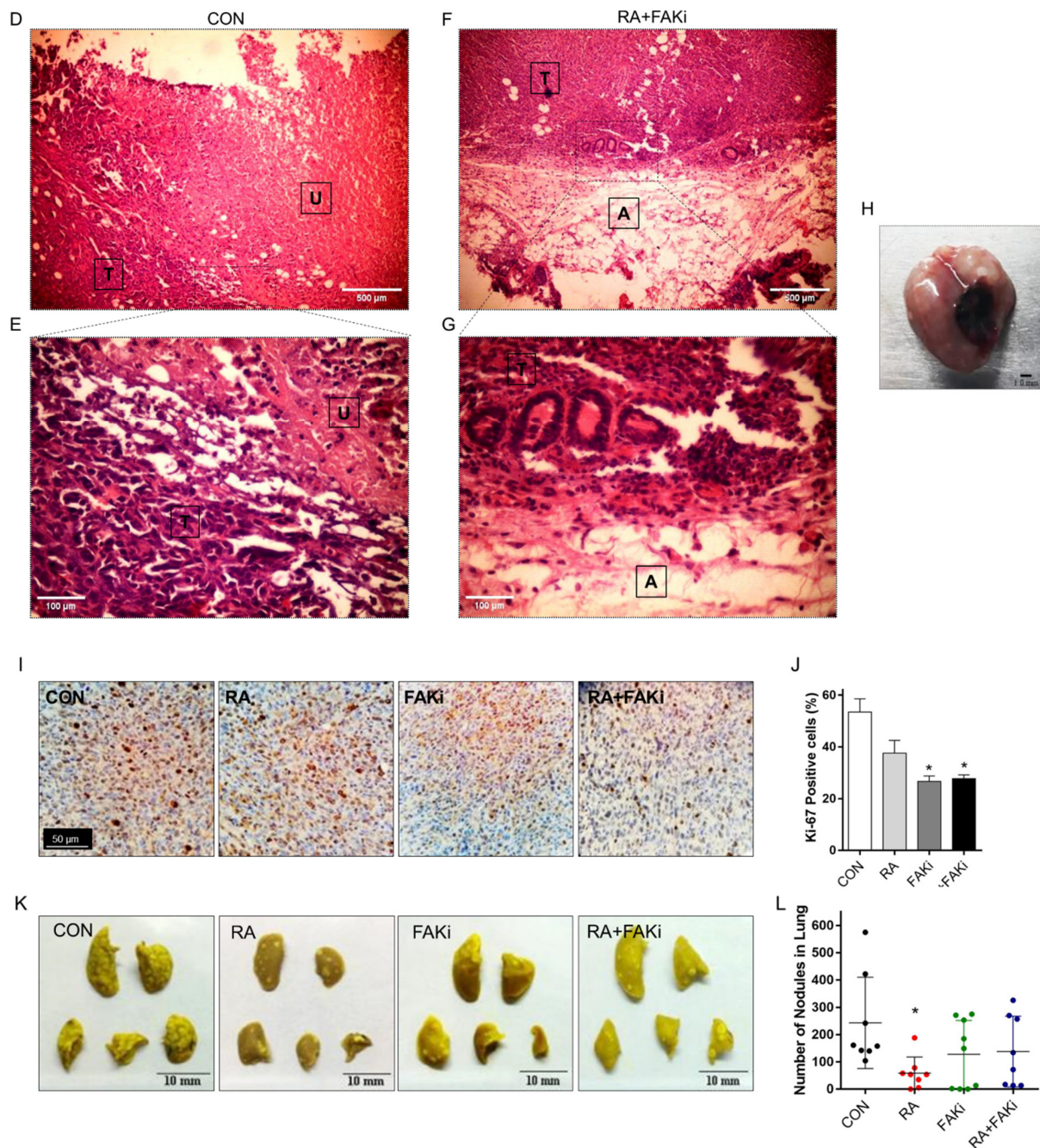


Figure 5. Cont.



**Figure 5.** Combination of RA plus FAKi in a murine experimental model. An orthotopic tumor growth assay was performed inoculating LM3 cells pretreated or not with FAKi (1  $\mu$ M, 72 h) into BALB/c mice. Animals also received a subcutaneous silastic pellet containing RA (10 mg) or an empty pellet. (A) Tumor diameters were measured twice a week and used to calculate tumor volume. Each data point represents the mean  $\pm$  SD, \* =  $p < 0.05$  vs. control, CON. (B) Representative images are shown. A dotted square indicates tumors. (C) Kaplan-Meier analysis of animal endpoint survival. Each color represents a different experimental group: control group (black), RA group (red), FAKi group (green), and RA + FAKi group (blue). (D–H) Effect of RA plus FAKi on histopathological features of LM3 orthotopic tumors. Tumors were fixed in 10% formalin and slides were stained with hematoxylin and eosin (T: Tumoral tissue, U: Ulcerated tissue, and A: Adipose tissue). (D,F) are images acquired at 100x magnification. (E,G) are the same sections with a 400 $\times$  magnification. (H) Representative image of an ulcerated tumor. (I,J) Images and the percentage of positive Ki-67-mammary tumor of LM3 cells compared to the control, CON; for each experimental condition are shown. \* =  $p < 0.05$  vs. control, CON. (K,L) An experimental metastasis assay was performed by

inoculating LM3 cells, pretreated or not with FAKi (1 $\mu$ M, 72 h), in the lateral tail vein of mice carrying a subcutaneous silastic pellet containing RA (10 mg) or an empty pellet. Twenty-one days post-inoculation, mice were sacrificed and the number of lung nodules was recorded. Each data point represents the number of lung nodules per animal. Each color denotes a different experimental group: control group (black), RA group (red), FAKi group (green), and RA + FAKi group (blue). Representative images are shown. The figure shows the results of one experiment representative of two independent assays. \* =  $p < 0.05$  vs. control, CON.

#### 4. Discussion

Although RA has demonstrated a potent anticancer activity, its use in solid tumors is limited by its controversial behavior, emphasizing the need for a better understanding of the RA molecular mechanism. Therefore, and taking into account that FAK is a pivotal kinase and scaffold protein that modulates cell adhesion and migration, processes involved in metastasis development, we evaluated whether a therapeutic approach based on RA administration combined with FAKi improves tumor progression inhibition.

A bioinformatics analysis and its subsequent validation by qPCR confirmed that the expression of SRC and PTK2 is high in BC cells. The overexpression of Src and FAK in many cancers is well established, and they are correlated with a poor prognosis for patients [19,38–40]. We also observed that RARA, encoding RAR $\alpha$ , the central receptor that mediates the antitumor activity of RA, was expressed at different levels within BC cells. This fact coincides with RA-sensitivity reported for BC cell lines, where SK-BR3 is considered RA-sensitive and MDA-MB-231 RA-resistant based on its high and low expression of RARA, respectively [41–43]. We also showed that RARB and RARG, encoding RAR $\beta$  and RAR $\gamma$  respectively, were uniformly and under-expressed in all BC. Similar results were obtained by Lu et al. (2005) [42]. This fact is not surprising since RAR $\beta$  has been reported to act as a tumor suppressor [44,45]. RAR $\beta$  is necessary to inhibit tumor proliferation and migration. The diminished RARB mRNA due to epigenetic alterations in BC has been widely demonstrated. It has been proposed as an epigenetic marker for BC diagnosis [26,46,47]. The role of RAR $\gamma$  has not been extensively studied in the context of BC.

In addition, we showed that VIM, MSN, TLN1, CTNNA1, CTTN, MMP9, and CDH2 (encoding vimentin, moesin, talin,  $\beta$ -catenin, cortactin, metalloprotease-9, and N-cadherin, respectively) are differentially expressed between RA-resistant and RA-sensitive BC cells. The functional products of these genes are directly or indirectly modulated by the Src-FAK complex through interactions to trigger the metastatic process [24,48].

In silico analysis and qPCR results in RA-resistant MDA-MB-231 and MDA-MB-468 BC cells showed that RA treatment regulated all genes tested despite being resistant to RA. Interestingly, RA downregulated VIM, MSN, and TLN1 genes previously demonstrated to be overexpressed in RA-resistant compared to RA-sensitive cells. In addition to these genes, RA reduced the expression of other genes involved in the adhesion/migration process, such as PXN, VCL, ACTR3, and PTK2. Despite lacking RARA receptors, and therefore being resistant to RA and insensitive to the RA-induced decrease in proliferation, RA could inhibit the adhesion, migration, invasion, and, consequently, metastasis by reducing the expression of target genes involved in these events. Coyle et al. (2017) provided evidence that RA, in addition to the widely studied canonical mechanism, governs the expression of a vast number of genes in a RARE-independent way through RA-inducible transcription factors [49]. The finding marker genes of RA response based on its differential expression in RA-sensitive vs. RA-resistant BC cells is promising not only in RA-sensitive cells but also in the treatment of triple-negative BC that currently lacks a specific therapy; however, more studies on this topic are needed to reach critical conclusions, and these results are beyond the scope of the manuscript.

Collectively, these data strongly support the idea that the combination of RA plus FAKi could improve the RA therapy in treating advanced-stage BC patients. Thus, we

next examined *in vitro* and *in vivo* the ability of RA + FAKi to inhibit BC progression. Numerous studies have found that RA reduces cell adhesion and migration in BC [26,27,50] and other types of cancer [51–53]. Our results confirm that RA inhibits cell adhesion and migration in T-47D, LM3, and HeLa cells. Disruption of cell adhesion and motility has also been reported after FAKi treatment in BC cells [54–57]. Our findings reveal that although RA and FAKi administered separately decrease adhesion and migration in LM3 BC cells, the novelty of our work is that their combination exerts a higher effect.

We also examined the ability of RA + FAKi on *in vitro* LM3 and T-47D cell viability and apoptosis. We noted a synergistic effect when RA (100  $\mu$ M) and FAKi (2  $\mu$ M) were combined. Although no studies evaluated this combination, several reports demonstrated that RA and FAKi administered separately inhibit BC cells' viability [58–61].

The anticancer effects of RA are mainly the result of growth inhibition with the subsequent induction of apoptosis. Several studies reported the induction of apoptosis after RA treatment [25,62,63]. Hong TK & Lee-Kim YC showed that RA (1  $\mu$ M, 4 days) induced apoptosis increasing caspase activity in MCF7 cells. They did not observe effects in RA-resistant MDA-MB-231 BC cells [64]. Similarly, in SK-BR3 BC cells, RA (1  $\mu$ M, 2–4 days) induces caspase-3 cleavage in a time- and dose-dependent manner [65]. Additionally, a vast bibliography affirmed that FAK inhibitors induce cancer apoptosis [21,66–68]. PND-1186, a FAKi, inhibited 4T1 breast carcinoma tumor growth, which correlated with elevated apoptosis and caspase-3 activation [68]. A different FAKi, GSK2256098, suppresses FAK downstream signaling pathways, inducing apoptosis via caspase-9/PARP [69]. Our results confirmed that in BC cells, treatments with RA, FAKi (2  $\mu$ M) and their combination induced an increase in the apoptosis markers active caspase-3 and cleaved PARP1.

When we assessed the expression of RARs, FAK and Paxillin by western blot, we observed that RA induces the downregulation of RAR $\alpha$ , FAK and Paxillin. Coadministration with FAKi improves this downregulation. We have previously reported that RA treatment (72 h) promotes FAK downregulation [26]. Similarly, Dutta et al. (2009 and 2010) have demonstrated that RA treatment (20–30  $\mu$ M, 24–48 h) on MDA-MB-231 and MCF-7 cells triggers the downregulation of FAK expression [70,71]. They also reported that the administration of RA increases RAR expression, but they did not differentiate between RAR isoforms [71].

We also study the phosphorylation/activation of FAK and its downstream protein Paxillin under our experimental conditions. We had previously reported that the administration of 1  $\mu$ M RA for short periods (20 min) increased the activation/phosphorylation of FAK and Paxillin, inducing their nuclear relocalization in T-47D breast cancer cells [27]. In the current study, we demonstrated that prolonged treatment with RA, FAKi, and their combination inhibit FAK and Paxillin phosphorylation, preventing their activation. These findings also confirmed the inhibitory mechanism of FAKi and that the inhibition of FAK and Paxillin persist after a long treatment (72 h).

One of the most intriguing actions of RA and FAKi is the control of the distribution and expression of FAK, overexpressed in the majority of breast cancer subtypes and critical for the invasion and metastasis process. In this work, we observed that RA and FAKi reduce FAK expression, achieving a higher diminishment when cells were exposed to the combined RA+FAKi treatment. Interestingly, we also provide evidence that RA, FAKi, and the combined treatment inhibit the relocalization of FAK to the plasmatic membrane, leaving cells with a static phenotype. This phenomenon was observed when the treatment of RA and RA+FAKi promoted nuclear FAK translocation. Our group and other colleagues have reported that the individual use of the RA and FAK inhibitor enables the FAK to shuttle between the cytoplasm and the nucleus [27,72–74]; however, the nuclear role of FAK is not completely clear. FAK in the cytoplasm controls proliferation, adhesion, migration, and invasion in a kinase-dependent manner, while FAK in the nucleus acts in a kinase-independent way to regulate gene expression [74]. We suggest that when FAK is not found at FAs, it is impossible to trigger the migratory and invasive processes. In agreement with

our previous findings, we propose an interesting regulatory mechanism in cell adhesion and migration, which are affected by the subcellular localization of FAK [27].

Another important finding of this work is the correlation between *in vitro* and *in vivo* results. In a murine BC model, we found that the administration of RA plus FAKi reduces tumor volume from the tenth day after orthotopic inoculation. Furthermore, we demonstrated that mice administered with the combined treatment enhanced their survival compared to the control group. In accordance with this, other authors have demonstrated that RA inhibits the growth of LM3, MDA-MB-231, and MCF-7 orthotopic tumors [75–77]. Furthermore, we showed that the exposition of mice to the combined treatment decreases Ki-67 expression, indicating a more differentiated state and a reduction in tumor cellular proliferation. This result is consistent with previous works that demonstrated the molecular actions of RA and FAKi promoting tumor cell differentiation [78–80].

Finally, we evaluated the ability of RA and FAKi to inhibit tumor cell dissemination. RA administered as a single agent was effective in interrupting the spread of cancer cells to the lung. Previously, other groups have reported the ability of RA to inhibit metastasis [81–83]. In contrast, Berardi et al. (2014) and Bessone et al. (2020) did not observe differences between the control and RA-treated groups [75,84]; however, they placed the RA patch five days before inoculation while we placed it one week previous to the injection. One interesting point to highlight is that FAK is inhibited during the first few days, 7–10 days approximately, at the time of tumor formation, and it has a negative effect on tumor growth. We suggested that FAK inhibition reduces adherence and the effective colonization of tumor cells. Cells that fail to adhere colonize and adapt to the new environment, die and do not participate in tumor formation, and tumor volume is reduced. The same is valid for the experimental metastasis assay; FAK is inhibited during the first few days, at the time of cell colonization, and cells that fail to colonize and adapt to the new environment die and do not form metastatic nodules.

In conclusion, our study reveals that RA-resistance would reflect the deregulation of most of the RA-target genes involved in cell adhesion, migration, and invasion, including genes encoding components of the Src-FAK dependent pathway. Our study demonstrates that RA and FAKi are essential in disrupting BC tumor growth and metastatic dissemination *in vitro* and *in vivo* by controlling FAK expression, phosphorylation/activation, and localization. FAKi impaired critical phosphorylation of FAK in residue Tyr 397, which serves as a canonical docking site for other signaling kinases and scaffolding proteins. Consequently, due to the impediment of protein interactions, a dissociation in the activation of downstream oncogenic pathways occurs. The blockade of FAK phosphorylation induces FAK detachment from FAs and its translocation to the nucleus. FAK acts as a transcription factor in a kinase-independent way to regulate target gene expression (Figure 6). Additionally, we show that RA, FAKi and their combination induce the expression of critical facilitators of apoptosis such as active-caspase-3 and cleaved-PARP1. Despite the complexity of the retinoid signaling in BC, the approach based on RA administered in combination with FAKi may be an effective strategy for treating metastatic patients since we demonstrated that RA sensibility could be exacerbated with FAKi coadministration. The combined treatment would inhibit the malignant phenotype in BC cells by disrupting cancer cell spread. Our findings also support the concept that the multifunctional protein FAK is a promising target for cancer therapy. Clinical trials are currently investigating treatment strategies using FAK inhibitors combined with chemotherapy, targeted therapy, or immunotherapy to increase FAKi efficacy [23]. Thus, selecting patients who could benefit from FAKi treatment alone or combination strategies would be essential.

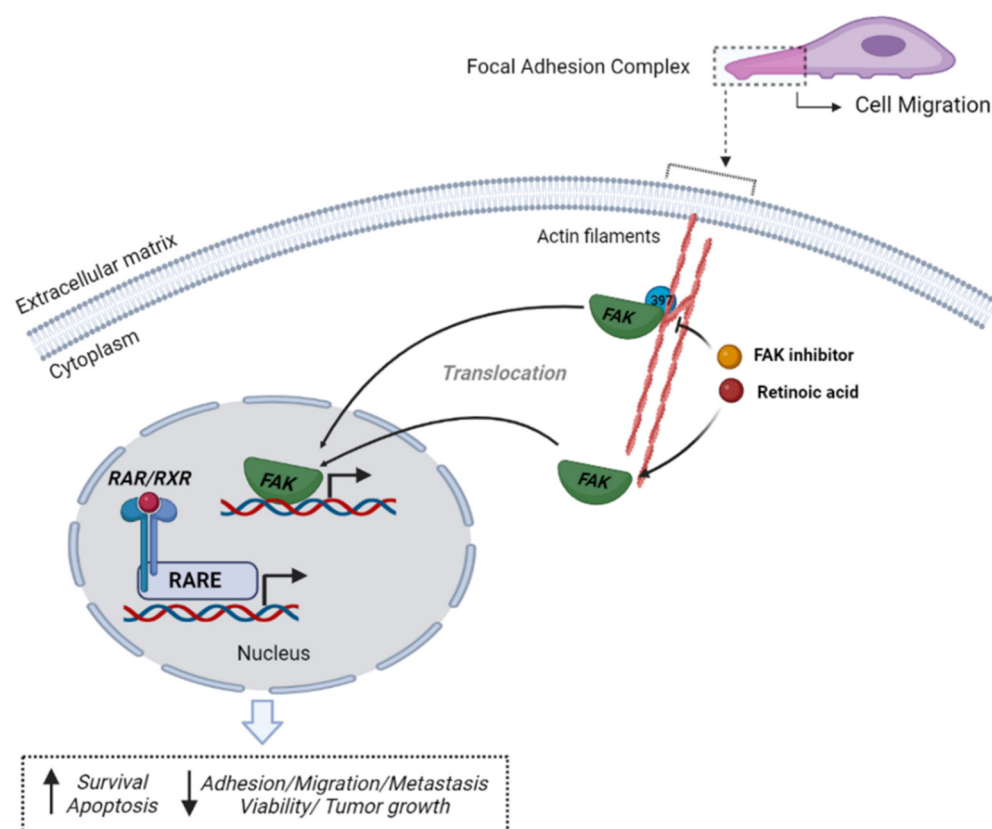


**Figure 6.** Schematic figure of molecular changes triggered by RA plus FAKi in BC. Retinoic acid (RA) and FAK inhibitor (FAKi) induces FAK translocation from focal adhesion sites and cytoplasm to the nucleus. In the nucleus, FAK acts as a transcription factor in a kinase-independent manner. In parallel, RA binds to receptors RXR/RARs regulating the transcription of target genes. As result, cell detachment occurs blocking cell migration and reducing the metastatic process. Likewise, cell viability diminished due to apoptosis induction decreasing tumor growth and increasing mice survival. Figure created by BioRender.

**Supplementary Materials:** The following supporting information can be downloaded at: <https://www.mdpi.com/article/10.3390/cells11192988/s1>.

**Author Contributions:** A.C.C.-G. carried out different experiments, cell culture, treatments and immunofluorescence assays. F.V. performed immunoblotting assays and Real-time quantitative PCR with reverse transcription. J.M.M. performed in vivo assays. J.M.F.-M. and F.C.M.Z. performed in silico analysis of RNA-Seq and microarray datasets. A.L.R. performed histology studies. A.M.S. was instrumental in funding the study and participated in the writing of the manuscript. M.I.F. planned and funded the project, supervised the experiments, wrote the manuscript. All authors have read and agreed to the published version of the manuscript.

**Funding:** This work has been financed by the *Agencia Nacional de Promoción Científica y Tecnológica* PICT-2015-0864 and PICT-2020-0512 to FMI; PICT-2015-2175 to AMS and by *Proyectos de Investigación de Unidades Ejecutoras* (PUE), Resolución No. 1547/16.

**Institutional Review Board Statement:** The animal study was reviewed and approved by the Institutional Animal Care and Use Committee of the School of Medical Science, Universidad Nacional de Cuyo, Mendoza, Argentina (Protocol approval N° 63/2015).

**Informed Consent Statement:** Not applicable.

**Data Availability Statement:** The original contributions presented in the study are included in the article/supplementary material. Further inquiries can be directed to the corresponding author(s).

**Acknowledgments:** The authors are grateful to Laura Todaro and Alejandro Urtreger for their excellent technical assistance with the in vivo experiments.

**Conflicts of Interest:** The authors have nothing to disclose. The authors declare that the research was conducted in the absence of any commercial or financial relationships that could be construed as a potential conflict of interest.

## References

1. Schenk, T.; Stengel, S.; Zelent, A. Unlocking the potential of retinoic acid in anticancer therapy. *Br. J. Cancer* **2014**, *111*, 2039–2045. [[CrossRef](#)]
2. Dobrotkova, V.; Chlapek, P.; Mazanek, P.; Sterba, J.; Veselska, R. Traffic lights for retinoids in oncology: Molecular markers of retinoid resistance and sensitivity and their use in the management of cancer differentiation therapy. *BMC Cancer* **2018**, *18*, 1059. [[CrossRef](#)]
3. Lalevee, S.; Anno, Y.N.; Chatagnon, A.; Samarut, E.; Poch, O.; Laudet, V.; Benoit, G.; Lecompte, O.; Rochette-Egly, C. Genome-wide in silico identification of new conserved and functional retinoic acid receptor response elements (direct repeats separated by 5 bp). *J. Biol. Chem.* **2011**, *286*, 33322–33334. [[CrossRef](#)]
4. Kumar, S.; Cunningham, T.J.; Duyster, G. Nuclear receptor corepressors Ncor1 and Ncor2 (Smrt) are required for retinoic acid-dependent repression of Fgf8 during somitogenesis. *Dev. Biol.* **2016**, *418*, 204–215. [[CrossRef](#)]
5. Chambon, P. A decade of molecular biology of retinoic acid receptors. *FASEB J.* **1996**, *10*, 940–954. [[CrossRef](#)]
6. Al Tanoury, Z.; Piskunov, A.; Rochette-Egly, C. Vitamin A and retinoid signaling: Genomic and nongenomic effects. *J. Lipid Res.* **2013**, *54*, 1761–1775. [[CrossRef](#)]
7. Giuli, M.V.; Hanieh, P.N.; Giuliani, E.; Rinaldi, F.; Marianecchi, C.; Screpanti, I.; Checquolo, S.; Carafa, M. Current Trends in ATRA Delivery for Cancer Therapy. *Pharmaceutics* **2020**, *12*, 707. [[CrossRef](#)]
8. Lo-Coco, F.; Avvisati, G.; Vignetti, M.; Thiede, C.; Orlando, S.M.; Iacobelli, S.; Ferrara, F.; Fazi, P.; Cicconi, L.; Di Bona, E.; et al. Retinoic acid and arsenic trioxide for acute promyelocytic leukemia. *N. Engl. J. Med.* **2013**, *369*, 111–121. [[CrossRef](#)]
9. Uray, I.P.; Dmitrovsky, E.; Brown, P.H. Retinoids and retinoids in cancer prevention: From laboratory to clinic. *Semin. Oncol.* **2016**, *43*, 49–64. [[CrossRef](#)]
10. Bushue, N.; Wan, Y.J. Retinoid pathway and cancer therapeutics. *Adv. Drug Deliv. Rev.* **2010**, *62*, 1285–1298. [[CrossRef](#)]
11. Garattini, E.; Bolis, M.; Garattini, S.K.; Fratelli, M.; Centritto, F.; Paroni, G.; Gianni, M.; Zanetti, A.; Pagani, A.; Fisher, J.N.; et al. Retinoids and breast cancer: From basic studies to the clinic and back again. *Cancer Treat. Rev.* **2014**, *40*, 739–749. [[CrossRef](#)]
12. Costantini, L.; Molinari, R.; Farinon, B.; Merendino, N. Retinoic Acids in the Treatment of Most Lethal Solid Cancers. *J. Clin. Med.* **2020**, *9*, 360. [[CrossRef](#)]
13. Gupta, G.P.; Massague, J. Cancer metastasis: Building a framework. *Cell* **2006**, *127*, 679–695. [[CrossRef](#)]
14. Singletary, S.E.; Connolly, J.L. Breast cancer staging: Working with the sixth edition of the AJCC Cancer Staging Manual. *CA Cancer J. Clin.* **2006**, *56*, 37–47; quiz 50–31. [[CrossRef](#)]
15. Nagano, M.; Hoshino, D.; Koshikawa, N.; Akizawa, T.; Seiki, M. Turnover of focal adhesions and cancer cell migration. *Int. J. Cell Biol.* **2012**, *2012*, 310616. [[CrossRef](#)]
16. Shortrede, J.E.; Uzair, I.D.; Neira, F.J.; Flamini, M.I.; Sanchez, A.M. Paxillin, a novel controller in the signaling of estrogen to FAK/N-WASP/Arp2/3 complex in breast cancer cells. *Mol. Cell. Endocrinol.* **2016**, *430*, 56–67. [[CrossRef](#)]
17. Zhao, X.; Guan, J.L. Focal adhesion kinase and its signaling pathways in cell migration and angiogenesis. *Adv. Drug Deliv. Rev.* **2011**, *63*, 610–615. [[CrossRef](#)]
18. Agochiya, M.; Brunton, V.G.; Owens, D.W.; Parkinson, E.K.; Paraskeva, C.; Keith, W.N.; Frame, M.C. Increased dosage and amplification of the focal adhesion kinase gene in human cancer cells. *Oncogene* **1999**, *18*, 5646–5653. [[CrossRef](#)] [[PubMed](#)]
19. Cance, W.G.; Harris, J.E.; Iacocca, M.V.; Roche, E.; Yang, X.; Chang, J.; Simkins, S.; Xu, L. Immunohistochemical analyses of focal adhesion kinase expression in benign and malignant human breast and colon tissues: Correlation with preinvasive and invasive phenotypes. *Clin. Cancer Res.* **2000**, *6*, 2417–2423. [[PubMed](#)]
20. Miyazaki, T.; Kato, H.; Nakajima, M.; Sohda, M.; Fukai, Y.; Masuda, N.; Manda, R.; Fukuchi, M.; Tsukada, K.; Kuwano, H. FAK overexpression is correlated with tumour invasiveness and lymph node metastasis in oesophageal squamous cell carcinoma. *Br. J. Cancer* **2003**, *89*, 140–145. [[CrossRef](#)]
21. Lv, P.C.; Jiang, A.Q.; Zhang, W.M.; Zhu, H.L. FAK inhibitors in Cancer, a patent review. *Expert Opin. Ther. Pat.* **2018**, *28*, 139–145. [[CrossRef](#)]
22. Schultze, A.; Fiedler, W. Therapeutic potential and limitations of new FAK inhibitors in the treatment of cancer. *Expert Opin. Investig. Drugs* **2010**, *19*, 777–788. [[CrossRef](#)]
23. Mohanty, A.; Pharaon, R.R.; Nam, A.; Salgia, S.; Kulkarni, P.; Massarelli, E. FAK-targeted and combination therapies for the treatment of cancer: An overview of phase I and II clinical trials. *Expert Opin. Investig. Drugs* **2020**, *29*, 399–409. [[CrossRef](#)]
24. Mousson, A.; Sick, E.; Carl, P.; Dujardin, D.; De Mey, J.; Ronde, P. Targeting Focal Adhesion Kinase Using Inhibitors of Protein-Protein Interactions. *Cancers* **2018**, *10*, 278. [[CrossRef](#)]

25. Berardi, D.E.; Ariza Bareno, L.; Amigo, N.; Canonero, L.; Pelagatti, M.L.N.; Motter, A.N.; Taruselli, M.A.; Diaz Bessone, M.I.; Cirigliano, S.M.; Edelstein, A.; et al. All-trans retinoic acid and protein kinase C alpha/beta1 inhibitor combined treatment targets cancer stem cells and impairs breast tumor progression. *Sci. Rep.* **2021**, *11*, 6044. [[CrossRef](#)]
26. Flamini, M.I.; Gauna, G.V.; Sottile, M.L.; Nadin, B.S.; Sanchez, A.M.; Vargas-Roig, L.M. Retinoic acid reduces migration of human breast cancer cells: Role of retinoic acid receptor beta. *J. Cell. Mol. Med.* **2014**, *18*, 1113–1123. [[CrossRef](#)]
27. Sanchez, A.M.; Shortrede, J.E.; Vargas-Roig, L.M.; Flamini, M.I. Retinoic acid induces nuclear FAK translocation and reduces breast cancer cell adhesion through Moesin, FAK, and Paxillin. *Mol. Cell. Endocrinol.* **2016**, *430*, 1–11. [[CrossRef](#)]
28. Vanderhoeven, F.; Redondo, A.L.; Martinez, A.L.; Vargas-Roig, L.M.; Sanchez, A.M.; Flamini, M.I. Synergistic antitumor activity by combining trastuzumab with retinoic acid in HER2 positive human breast cancer cells. *Oncotarget* **2018**, *9*, 26527–26542. [[CrossRef](#)]
29. Urtreger, A.; Ladeda, V.; Puricelli, L.; Rivelli, A.; Vidal, M.; Delustig, E.; Joffe, E. Modulation of fibronectin expression and proteolytic activity associated with the invasive and metastatic phenotype in two new murine mammary tumor cell lines. *Int. J. Oncol.* **1997**, *11*, 489–496. [[CrossRef](#)]
30. Davis, S.; Meltzer, P.S. GEOquery: A bridge between the Gene Expression Omnibus (GEO) and BioConductor. *Bioinformatics* **2007**, *23*, 1846–1847. [[CrossRef](#)]
31. Johnson, W.E.; Li, C.; Rabinovic, A. Adjusting batch effects in microarray expression data using empirical Bayes methods. *Biostatistics* **2007**, *8*, 118–127. [[CrossRef](#)]
32. Leek, J.T.; Johnson, W.E.; Parker, H.S.; Jaffe, A.E.; Storey, J.D. The sva package for removing batch effects and other unwanted variation in high-throughput experiments. *Bioinformatics* **2012**, *28*, 882–883. [[CrossRef](#)]
33. Ritchie, M.E.; Phipson, B.; Wu, D.; Hu, Y.; Law, C.W.; Shi, W.; Smyth, G.K. limma powers differential expression analyses for RNA-sequencing and microarray studies. *Nucleic Acids Res.* **2015**, *43*, e47. [[CrossRef](#)]
34. Untergasser, A.; Ruijter, J.M.; Benes, V.; van den Hoff, M.J.B. Web-based LinRegPCR: Application for the visualization and analysis of (RT)-qPCR amplification and melting data. *BMC Bioinform.* **2021**, *22*, 1–18. [[CrossRef](#)]
35. Chou, T.C. Theoretical basis, experimental design, and computerized simulation of synergism and antagonism in drug combination studies. *Pharm. Rev.* **2006**, *58*, 621–681. [[CrossRef](#)]
36. Chou, T.C. Drug combination studies and their synergy quantification using the Chou-Talalay method. *Cancer Res.* **2010**, *70*, 440–446. [[CrossRef](#)]
37. Kelley, J.B.; Paschal, B.M. Fluorescence-based quantification of nucleocytoplasmic transport. *Methods* **2019**, *157*, 106–114. [[CrossRef](#)]
38. Zou, D.; Yoon, H.S.; Anjomshoaa, A.; Perez, D.; Fukuzawa, R.; Guilford, P.; Humar, B. Increased levels of active c-Src distinguish invasive from in situ lobular lesions. *Breast Cancer Res.* **2009**, *11*, R45. [[CrossRef](#)]
39. Elsberger, B.; Fullerton, R.; Zino, S.; Jordan, F.; Mitchell, T.J.; Brunton, V.G.; Mallon, E.A.; Shiels, P.G.; Edwards, J. Breast cancer patients' clinical outcome measures are associated with Src kinase family member expression. *Br. J. Cancer* **2010**, *103*, 899–909. [[CrossRef](#)]
40. Lark, A.L.; Livasy, C.A.; Dressler, L.; Moore, D.T.; Millikan, R.C.; Geradts, J.; Iacocca, M.; Cowan, D.; Little, D.; Craven, R.J.; et al. High focal adhesion kinase expression in invasive breast carcinomas is associated with an aggressive phenotype. *Mod. Pathol.* **2005**, *18*, 1289–1294. [[CrossRef](#)]
41. Centritto, F.; Paroni, G.; Bolis, M.; Garattini, S.K.; Kurosaki, M.; Barzago, M.M.; Zanetti, A.; Fisher, J.N.; Scott, M.F.; Pattini, L.; et al. Cellular and molecular determinants of all-trans retinoic acid sensitivity in breast cancer: Luminal phenotype and RARalpha expression. *EMBO Mol. Med.* **2015**, *7*, 950–972. [[CrossRef](#)] [[PubMed](#)]
42. Lu, M.; Mira-y-Lopez, R.; Nakajo, S.; Nakaya, K.; Jing, Y. Expression of estrogen receptor alpha, retinoic acid receptor alpha and cellular retinoic acid binding protein II genes is coordinately regulated in human breast cancer cells. *Oncogene* **2005**, *24*, 4362–4369. [[CrossRef](#)]
43. Schneider, S.M.; Offterdinger, M.; Huber, H.; Grunt, T.W. Activation of retinoic acid receptor alpha is sufficient for full induction of retinoid responses in SK-BR-3 and T47D human breast cancer cells. *Cancer Res.* **2000**, *60*, 5479–5487.
44. Sun, S.Y.; Wan, H.; Yue, P.; Hong, W.K.; Lotan, R. Evidence that retinoic acid receptor beta induction by retinoids is important for tumor cell growth inhibition. *J. Biol. Chem.* **2000**, *275*, 17149–17153. [[CrossRef](#)]
45. Xu, Q.; Jitkaew, S.; Choksi, S.; Kadigamuwa, C.; Qu, J.; Choe, M.; Jang, J.; Liu, C.; Liu, Z.G. The cytoplasmic nuclear receptor RARgamma controls RIP1 initiated cell death when cIAP activity is inhibited. *Nat. Commun.* **2017**, *8*, 425. [[CrossRef](#)] [[PubMed](#)]
46. Fang, C.; Jian, Z.Y.; Shen, X.F.; Wei, X.M.; Yu, G.Z.; Zeng, X.T. Promoter Methylation of the Retinoic Acid Receptor Beta2 (RARbeta2) Is Associated with Increased Risk of Breast Cancer: A PRISMA Compliant Meta-Analysis. *PLoS ONE* **2015**, *10*, e0140329. [[CrossRef](#)]
47. Yari, K.; Rahimi, Z. Promoter Methylation Status of the Retinoic Acid Receptor-Beta 2 Gene in Breast Cancer Patients: A Case Control Study and Systematic Review. *Breast Care* **2019**, *14*, 117–123. [[CrossRef](#)] [[PubMed](#)]
48. Zhao, J.; Guan, J.L. Signal transduction by focal adhesion kinase in cancer. *Cancer Metastasis Rev.* **2009**, *28*, 35–49. [[CrossRef](#)] [[PubMed](#)]
49. Coyle, K.M.; Maxwell, S.; Thomas, M.L.; Marcato, P. Profiling of the transcriptional response to all-trans retinoic acid in breast cancer cells reveals RARE-independent mechanisms of gene expression. *Sci. Rep.* **2017**, *7*, 16684. [[CrossRef](#)] [[PubMed](#)]

50. Zanetti, A.; Affatato, R.; Centritto, F.; Fratelli, M.; Kurosaki, M.; Barzago, M.M.; Bolis, M.; Terao, M.; Garattini, E.; Paroni, G. All-trans-retinoic Acid Modulates the Plasticity and Inhibits the Motility of Breast Cancer Cells: Role of NOTCH1 and Transforming Growth Factor (TGFbeta). *J. Biol. Chem.* **2015**, *290*, 17690–17709. [[CrossRef](#)]
51. Cui, J.; Gong, M.; He, Y.; Li, Q.; He, T.; Bi, Y. All-trans retinoic acid inhibits proliferation, migration, invasion and induces differentiation of hepa1-6 cells through reversing EMT in vitro. *Int. J. Oncol.* **2016**, *48*, 349–357. [[CrossRef](#)]
52. Woo, Y.J.; Jang, K.L. All-trans retinoic acid activates E-cadherin expression via promoter hypomethylation in the human colon carcinoma HCT116 cells. *Biochem. Biophys. Res. Commun.* **2012**, *425*, 944–949. [[CrossRef](#)]
53. Zuo, L.; Yang, X.; Lu, M.; Hu, R.; Zhu, H.; Zhang, S.; Zhou, Q.; Chen, F.; Gui, S.; Wang, Y. All-Trans Retinoic Acid Inhibits Human Colorectal Cancer Cells RKO Migration via Downregulating Myosin Light Chain Kinase Expression through MAPK Signaling Pathway. *Nutr. Cancer* **2016**, *68*, 1225–1233. [[CrossRef](#)]
54. Chauhan, A.; Khan, T. Focal adhesion kinase—An emerging viable target in cancer and development of focal adhesion kinase inhibitors. *Chem. Biol. Drug Des.* **2021**, *97*, 774–794. [[CrossRef](#)]
55. Hao, H.; Naomoto, Y.; Bao, X.; Watanabe, N.; Sakurama, K.; Noma, K.; Motoki, T.; Tomono, Y.; Fukazawa, T.; Shirakawa, Y.; et al. Focal adhesion kinase as potential target for cancer therapy (Review). *Oncol. Rep.* **2009**, *22*, 973–979.
56. Lu, Y.; Sun, H. Progress in the Development of Small Molecular Inhibitors of Focal Adhesion Kinase (FAK). *J. Med. Chem.* **2020**, *63*, 14382–14403. [[CrossRef](#)]
57. Parsons, J.T.; Slack-Davis, J.; Tilghman, R.; Roberts, W.G. Focal adhesion kinase: Targeting adhesion signaling pathways for therapeutic intervention. *Clin. Cancer Res.* **2008**, *14*, 627–632. [[CrossRef](#)]
58. Van Heusden, J.; Wouters, W.; Ramaekers, F.C.; Krekels, M.D.; Dillen, L.; Borgers, M.; Smets, G. All-trans-retinoic acid metabolites significantly inhibit the proliferation of MCF-7 human breast cancer cells in vitro. *Br. J. Cancer* **1998**, *77*, 26–32. [[CrossRef](#)]
59. Golubovskaya, V.M.; Figel, S.; Ho, B.T.; Johnson, C.P.; Yemma, M.; Huang, G.; Zheng, M.; Nyberg, C.; Magis, A.; Ostrov, D.A.; et al. A small molecule focal adhesion kinase (FAK) inhibitor, targeting Y397 site: 1-(2-hydroxyethyl)-3, 5, 7-triaza-1-azoniatricyclo [3.3.1.1(3,7)] decane; bromide effectively inhibits FAK autophosphorylation activity and decreases cancer cell viability, clonogenicity and tumor growth in vivo. *Carcinogenesis* **2012**, *33*, 1004–1013. [[CrossRef](#)]
60. Walsh, C.; Tanjoni, I.; Uryu, S.; Tomar, A.; Nam, J.O.; Luo, H.; Phillips, A.; Patel, N.; Kwok, C.; McMahon, G.; et al. Oral delivery of PND-1186 FAK inhibitor decreases tumor growth and spontaneous breast to lung metastasis in pre-clinical models. *Cancer Biol.* **2010**, *9*, 778–790. [[CrossRef](#)]
61. Toma, S.; Isnardi, L.; Raffo, P.; Dastoli, G.; De Francisci, E.; Riccardi, L.; Palumbo, R.; Bollag, W. Effects of all-trans-retinoic acid and 13-cis-retinoic acid on breast-cancer cell lines: Growth inhibition and apoptosis induction. *Int. J. Cancer* **1997**, *70*, 619–627. [[CrossRef](#)]
62. Abdolahi, M.; Shokri, F.; Hosseini, M.; Shadani, M.; Saboor-Yaraghi, A.A. The combined effects of all-trans-retinoic acid and docosahexaenoic acid on the induction of apoptosis in human breast cancer MCF-7 cells. *J. Cancer Res. Ther.* **2016**, *12*, 204–208. [[CrossRef](#)]
63. Koay, D.C.; Zerillo, C.; Narayan, M.; Harris, L.N.; DiGiovanna, M.P. Anti-tumor effects of retinoids combined with trastuzumab or tamoxifen in breast cancer cells: Induction of apoptosis by retinoid/trastuzumab combinations. *Breast Cancer Res.* **2010**, *12*, R62. [[CrossRef](#)]
64. Hong, T.K.; Lee-Kim, Y.C. Effects of retinoic acid isomers on apoptosis and enzymatic antioxidant system in human breast cancer cells. *Nutr. Res. Pract.* **2009**, *3*, 77–83. [[CrossRef](#)]
65. Brigger, D.; Schlafli, A.M.; Garattini, E.; Tschan, M.P. Activation of RARalpha induces autophagy in SKBR3 breast cancer cells and depletion of key autophagy genes enhances ATRA toxicity. *Cell Death Dis.* **2015**, *6*, e1861. [[CrossRef](#)] [[PubMed](#)]
66. Golubovskaya, V.M.; Gross, S.; Kaur, A.S.; Wilson, R.I.; Xu, L.H.; Yang, X.H.; Cance, W.G. Simultaneous inhibition of focal adhesion kinase and SRC enhances detachment and apoptosis in colon cancer cell lines. *Mol. Cancer Res. MCR* **2003**, *1*, 755–764.
67. Golubovskaya, V.M.; Virnig, C.; Cance, W.G. TAE226-induced apoptosis in breast cancer cells with overexpressed Src or EGFR. *Mol. Carcinog.* **2008**, *47*, 222–234. [[CrossRef](#)]
68. Tanjoni, I.; Walsh, C.; Uryu, S.; Tomar, A.; Nam, J.O.; Mielgo, A.; Lim, S.T.; Liang, C.; Koenig, M.; Sun, C.; et al. PND-1186 FAK inhibitor selectively promotes tumor cell apoptosis in three-dimensional environments. *Cancer Biol. Ther.* **2010**, *9*, 764–777. [[CrossRef](#)] [[PubMed](#)]
69. Zhang, J.; He, D.H.; Zajac-Kaye, M.; Hochwald, S.N. A small molecule FAK kinase inhibitor, GSK2256098, inhibits growth and survival of pancreatic ductal adenocarcinoma cells. *Cell Cycle* **2014**, *13*, 3143–3149. [[CrossRef](#)]
70. Dutta, A.; Sen, T.; Banerji, A.; Das, S.; Chatterjee, A. Studies on Multifunctional Effect of All-Trans Retinoic Acid (ATRA) on Matrix Metalloproteinase-2 (MMP-2) and Its Regulatory Molecules in Human Breast Cancer Cells (MCF-7). *J. Oncol.* **2009**, *2009*, 627840. [[CrossRef](#)]
71. Dutta, A.; Sen, T.; Chatterjee, A. All-trans retinoic acid (ATRA) downregulates MMP-9 by modulating its regulatory molecules. *Cell Adhes. Migr.* **2010**, *4*, 409–418. [[CrossRef](#)] [[PubMed](#)]
72. Lietha, D.; Cai, X.; Ceccarelli, D.F.; Li, Y.; Schaller, M.D.; Eck, M.J. Structural basis for the autoinhibition of focal adhesion kinase. *Cell* **2007**, *129*, 1177–1187. [[CrossRef](#)]
73. Lim, S.T.; Chen, X.L.; Lim, Y.; Hanson, D.A.; Vo, T.T.; Howerton, K.; Larocque, N.; Fisher, S.J.; Schlaepfer, D.D.; Ilic, D. Nuclear FAK promotes cell proliferation and survival through FERM-enhanced p53 degradation. *Mol. Cell* **2008**, *29*, 9–22. [[CrossRef](#)]

74. Zhou, J.; Yi, Q.; Tang, L. The roles of nuclear focal adhesion kinase (FAK) on Cancer: A focused review. *J. Exp. Clin. Cancer Res.* **2019**, *38*, 250. [[CrossRef](#)]
75. Berardi, D.E.; Bessone, M.I.; Motter, A.; Bal de Kier Joffe, E.D.; Urtreger, A.J.; Todaro, L.B. Involvement of protein kinase C alpha and delta activities on the induction of the retinoic acid system in mammary cancer cells. *Mol. Carcinog.* **2015**, *54*, 1110–1121. [[CrossRef](#)]
76. Huang, S.; Chen, Y.; Liang, Z.M.; Li, N.N.; Liu, Y.; Zhu, Y.; Liao, D.; Zhou, X.Z.; Lu, K.P.; Yao, Y.; et al. Targeting Pin1 by All-Trans Retinoic Acid (ATRA) Overcomes Tamoxifen Resistance in Breast Cancer via Multifactorial Mechanisms. *Front. Cell Dev. Biol.* **2019**, *7*, 322. [[CrossRef](#)]
77. Wei, S.; Kozono, S.; Kats, L.; Nechama, M.; Li, W.; Guarnerio, J.; Luo, M.; You, M.H.; Yao, Y.; Kondo, A.; et al. Active Pin1 is a key target of all-trans retinoic acid in acute promyelocytic leukemia and breast cancer. *Nat. Med.* **2015**, *21*, 457–466. [[CrossRef](#)]
78. Gudas, L.J.; Wagner, J.A. Retinoids regulate stem cell differentiation. *J. Cell. Physiol.* **2011**, *226*, 322–330. [[CrossRef](#)]
79. Kolev, V.N.; Tam, W.F.; Wright, Q.G.; McDermott, S.P.; Vidal, C.M.; Shapiro, I.M.; Xu, Q.; Wicha, M.S.; Pachter, J.A.; Weaver, D.T. Inhibition of FAK kinase activity preferentially targets cancer stem cells. *Oncotarget* **2017**, *8*, 51733–51747. [[CrossRef](#)]
80. Luo, M.; Fan, H.; Nagy, T.; Wei, H.; Wang, C.; Liu, S.; Wicha, M.S.; Guan, J.L. Mammary epithelial-specific ablation of the focal adhesion kinase suppresses mammary tumorigenesis by affecting mammary cancer stem/progenitor cells. *Cancer Res.* **2009**, *69*, 466–474. [[CrossRef](#)]
81. Chansri, N.; Kawakami, S.; Yamashita, F.; Hashida, M. Inhibition of liver metastasis by all-trans retinoic acid incorporated into O/W emulsions in mice. *Int. J. Pharm.* **2006**, *321*, 42–49. [[CrossRef](#)] [[PubMed](#)]
82. Zhou, Q.; Xian, M.; Xiang, S.; Xiang, D.; Shao, X.; Wang, J.; Cao, J.; Yang, X.; Yang, B.; Ying, M.; et al. All-Trans Retinoic Acid Prevents Osteosarcoma Metastasis by Inhibiting M2 Polarization of Tumor-Associated Macrophages. *Cancer Immunol. Res.* **2017**, *5*, 547–559. [[CrossRef](#)]
83. Grace, V.M.B.; Saranya, S.; Wilson, D.D. Protective role of All Trans Retinoic Acid on B16F10 melanoma cell line metastasis in C57BL/6 mice by enhancing RAR- beta protein and homeostasis maintenance. *J. Histotechnol.* **2021**, *44*, 127–138. [[CrossRef](#)] [[PubMed](#)]
84. Bessone, M.I.D.; Berardi, D.E.; Cirigliano, S.M.; Delbart, D.I.; Peters, M.G.; Todaro, L.B.; Urtreger, A.J. Protein Kinase C Alpha (PKCalpha) overexpression leads to a better response to retinoid acid therapy through Retinoic Acid Receptor Beta (RARbeta) activation in mammary cancer cells. *J. Cancer Res. Clin. Oncol.* **2020**, *146*, 3241–3253. [[CrossRef](#)] [[PubMed](#)]